

N87-18948

CONVECTIVE CELL DEVELOPMENT AND PROPAGATION
IN A MESOSCALE CONVECTIVE COMPLEX

Yoo-Shin Ahn

and

Kenneth C. Brundidge

Texas A & M University

College Station, Texas

Prepared for George C. Marshall Space Flight Center

under Contract NAG 8-043

ABSTRACT

A case study was made of the mesoscale convective complex (MCC) which occurred over southern Oklahoma and northern Texas on 27 May 1981. This storm moved in an eastsoutheasterly direction and during much of its lifetime was observable by radars at Oklahoma City, OK. and Stephenville, TX. It was found that the direction of cell (VIP level 3 or more reflectivity) propagation was somewhat erratic but approximately the same as the system (VIP level 1 reflectivity) movement and the ambient wind. New cells developed along and behind the gust front making it appear that once the MCC is initiated, a synergistic relationship exists between the gust front and the MCC. The relationship between rainfall patterns and amounts and the infrared (IR) temperature field in the satellite imagery were examined. The 210°K isotherm of GOES IR imagery was found to encompass the rain area of the storm. The heaviest rainfall was in the vicinity of the VIP level 3 cells and mostly contained within the 205°K isotherm of GOES IR imagery.

ACKNOWLEDGEMENTS

The authors are grateful the support for this work provided by the George C. Marshall Space Flight Center under Grant NAG. 8-043.

TABLE OF CONTENTS

	Page
ABSTRACT-----	11
ACKNOWLEDGEMENTS-----	111
TABLE OF CONTENTS-----	iv
LIST OF TABLES-----	v
LIST OF FIGURES-----	vi
I. INTRODUCTION-----	1
II. RESEARCH PROCEDURES-----	7
III. SYNOPTIC CONDITIONS AND STORM HISTORY-----	12
IV. STORM MOTION-----	19
V. NEW CELL DEVELOPMENT-----	30
VI. RADAR DATA DETAILS-----	33
VII. COMBINATION OF SATELLITE IMAGERY AND RADAR OBSERVATION-----	43
VIII. CONCLUSIONS AND RECOMMENDATIONS-----	50
REFERENCES-----	53

LIST OF TABLES

TABLE		Page
1	Mesoscale convective complex (MCC) definition-----	3
2	Description of manually digitized radar (MDR) code-----	8
3	Characteristics associated with the MCC of 27 May 1981-----	18

LIST OF FIGURES

FIGURE		Page
1	Schematic models of multi-cell storm propagation-----	5
2	The climatological network of raingauges in Texas-----	9
3	The climatological network of raingauges in Oklahoma-----	10
4	Synoptic analysis at 70 kPa for 0000 GMT, 27 May 1981-----	13
5	Synoptic analysis at 50 kPa for 0000 GMT, 27 May 1981-----	14
6	Surface synoptic analysis at 1400 GMT, 27 May 1981-----	16
7	GOES visible image for 1500 GMT, 27 May 1981-----	17
8a	VIP level 1 cell outlines at hourly intervals from 0000 to 0800 GMT-----	20
8b	VIP level 1 cell outlines at hourly intervals from 0901 to 1558 GMT-----	21
9a	VIP level 3 cell outlines at 20 min intervals from 0120 to 0700 GMT-----	23
9b	VIP level 3 cell outlines at 20 min intervals from 0721 to 1240 GMT-----	24
10	Hodographs at 1200 GMT for OKC (solid) and SEP (dashed)-----	26
11	VIP level 1 cell centroid positions at hourly intervals from 0000 to 1558 GMT-----	28
12	Gust front and VIP level 3 cell positions at hourly intervals-----	31
13	Combined VIP level 1 and level 3 radar echoes at hourly intervals from 0100 to 1558 GMT-----	34

14	Simultaneous views of satellite imagery and radar echoes at 0700 GMT-----	44
15	Simultaneous views of satellite imagery and radar echoes at 0800 GMT-----	46
16	Simultaneous views of satellite imagery and radar echoes at 0900 GMT-----	47
17	Simultaneous views of satellite imagery and radar echoes at 1000 GMT-----	48
18	Simultaneous views of satellite imagery and radar echoes at 1200 GMT-----	49

I. INTRODUCTION

For many years, meteorologists had believed that thunderstorms occurred in two basic forms: air mass storms represented by isolated cells and squall lines involving many cells organized into a line. However, as pointed out by Purdom (1979), the advent of the Geostationary Operational Environmental Satellite (GOES) has enabled meteorologists generally to see a variety of atmospheric events not distinguishable by ordinary synoptic observations. In particular, a third mode of thunderstorm activity has been recently discovered. It has been found that many summertime storms are organized aggregations of thunderstorm cells which Maddox (1980b) has called mesoscale convective complexes (MCCs).

Through examination of satellite imagery it has been found that thirty or more MCCs may occur in the United States during the months March through September (Maddox, 1980b; Maddox et al., 1982; Merritt and Fritsch, 1984; Rodgers et al., 1983; Rodgers et al., 1985). These systems may produce severe weather such as hail, tornadoes, damaging winds and flash flooding (Bosart and Sanders, 1981); however, they also have been found to be the main source of summertime rainfall over the crop lands of the mid-west (Fritsch et al., 1981).

MCCs have a distinctive appearance in satellite imagery. They appear as a nearly circular mass of cloud covering an area of 100,000 km² or more and at a temperature less than or equal to -32°C. The complete definition of an MCC is presented in Table 1. Whereas they may start in

the afternoon or evening MCCs primarily are nocturnal systems which reach maximum intensity sometime after midnight and may not dissipate until after sunrise (Maddox, 1980a). Frequently during the dissipating stage, the MCC produces an arc cloud (Purdom, 1973, 1976; Gurka, 1976) which moves outward from the MCC and may play a role in new storm development the following day.

The problem of understanding the movement and internal dynamics of thunderstorms and thunderstorm systems has been the subject of much research of the years. Byers and Braham (1949) found that small radar echoes moved with the cloud layer-mean wind. However, Zehr and Purdom (1982) did not find this wind to be a reliable indicator of storm motion. Newton and Fankhauser (1975) studied storm motion as related to storm size. They found that small- to medium-sized storms generally move to the left of the mean vector wind in the troposphere while large storms with diameters of about 20-30 km generally move to the right of the mean wind.

Observational studies which have been made of multi-cell systems (Fujita and Brown, 1958; Heymsfield and Schotz, 1985; Marwitz, 1972) have shown that such systems simultaneously move and maintain themselves by a process called "discrete propagation". In this process, new cells develop on the right flank of the storm area and move toward the left flank where they dissipate. This produces a complex of cells which as a whole moves to the right of the individual cell motion. Figure 1 shows three distinct propagation models as described by Marwitz (1972) for three different multi-cell storm systems. In Fig. 1a, the individual

TABLE 1. Mesoscale Convective Complex (MCC) definition.
The definition is based upon analysis of enhanced IR
satellite imagery (after Maddox, 1980b).

Physical Characteristics

Size: A: Cloud shield with IR temperature $\leq -32^{\circ}\text{C}$ must
 have an area $\geq 100,000 \text{ km}^2$
 B Interior cold cloud region with temperature
 $\leq -52^{\circ}\text{C}$ must have an area $\geq 50,000 \text{ km}^2$

Initiate: Size definitions A and B are first satisfied

Duration: Size definitions A and B must be met for a period
 $\geq 6 \text{ h}$

Maximum Contiguous cold cloud shield (IR temperature $\leq -32^{\circ}\text{C}$)
extent: reaches maximum size

Shape: Eccentricity (minor axis/major axis) ≥ 0.7 at time
 of maximum extent

Terminate: Size definitions A and B are no longer satisfied

whole cells, represented by ovals, propagate continuously in the direction of the mean wind coupled with discrete propagation to the right of the mean wind. The cells in Fig. 1b propagate both continuously and discretely to the right of the mean wind, which provides a large angular departure of storm motion from the mean wind. The third possibility in Fig. 1c is one in which continuous propagation is to the left of the mean wind but the offsetting discrete propagation to the right results in overall storm motion in the same direction as the mean wind. Numerical simulation studies such as those by Miller (1978) and Wilhelmson and Chen (1982) also show the tendency for discrete propagation to control storm motion. As pointed out by Wilhelmson and Chen, how the individual cells move relative to the mean vector wind in the cloud layer bears on the rate at which moisture can be supplied to them for continued growth.

The studies of multi-cell systems cited above did not involve the use of satellite imagery. Therefore, it is not clear to what extent the results may be applicable to MCCs which, as noted before, are defined on the basis of satellite imagery using criteria developed by Maddox (1980b). MCCs are large enough in scale to generally encompass several observing sites at any given time; however, the internal processes are sub-synoptic and therefore not easily determined. It is safe to say that these processes are poorly understood. Several questions may be asked:

- a. How are MCCs maintained during the nighttime hours when no surface heating is occurring to destabilize the boundary layer?

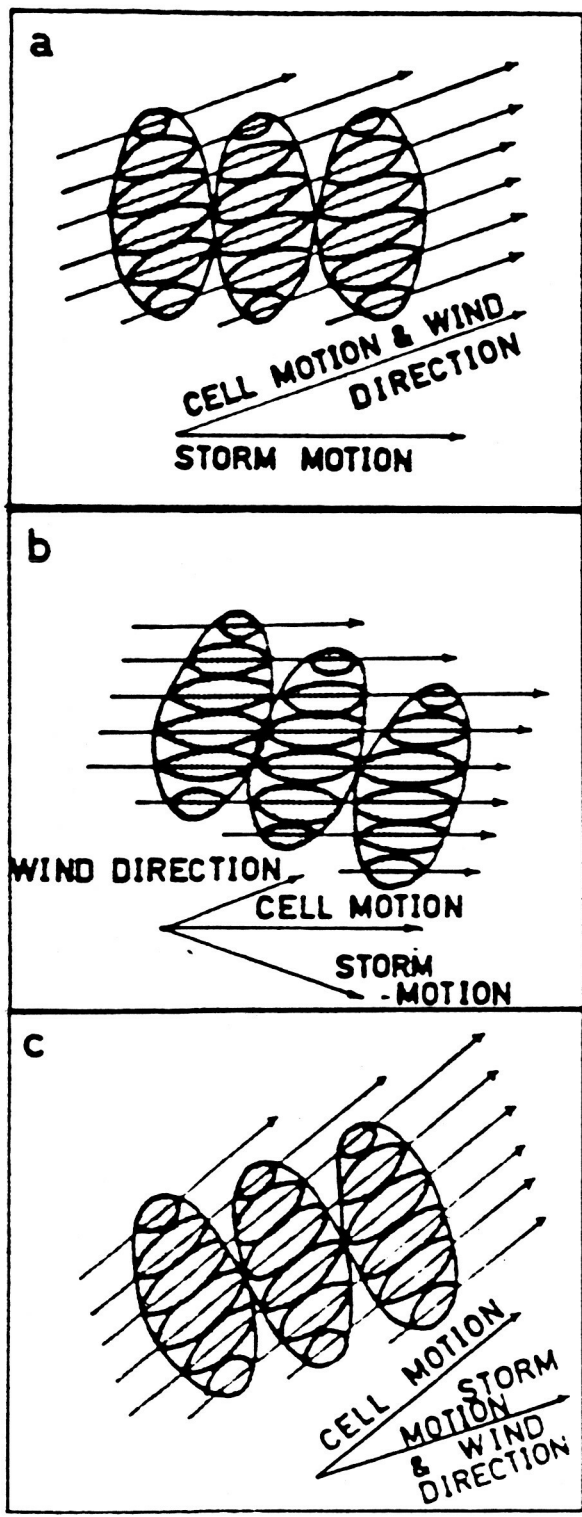


Fig. 1. Schematic models of multi-cell storm propagation (from Marwitz, 1972).

b. Do new cells develop on the interior of an MCC in a random fashion at the intersections of outflow boundaries, as occurs with air mass storms? Or is cell development related to the meso- β scale outflow boundary of the system as a whole?

c. How do the movement of individual cells and the movement of the system as a whole relate to one another and to the mean cloud-layer wind?

At present, answers to these questions can only be inferred from inadequate observations. Maddox and Howard (1983) have urged the use of satellite imagery and radar observations in combination to obtain a better understanding of the precipitation structure of middle-latitude mesosystems, to improve understanding of the life cycle of MCCs as an aid to forecasting them, and to provide better estimates of rainfall patterns and amounts based on cloud-top IR temperature structure. The study described here was this approach to focus on the problem areas described above in a case study of the MCC which occurred over southern Oklahoma and northern Texas on 27 May 1981. This storm moved in a southeasterly direction and during much of its lifetime was observed simultaneously by radars at Oklahoma City (OKC), OK. and Stephenville (SEP), TX.

II. RESEARCH PROCEDURES

The data used and the procedures followed in this study are as follows.

a Radar films for 27 May 1981 for the OKC and SEP radar sites were obtained from the National Climatic Data Center, Asheville, North Carolina. These films, with frames at one minute intervals, were examined to determine the history of cell development and movement. For this purpose a "cell" was defined to be a reflectivity region at a Video Integrator Processor (VIP) level of 3 or more. The system as a whole was defined as all the area enclosed by the VIP level 1 reflectivity value. The relationships between the manually digitized radar (MDR) code, which is used for the hourly radar summary maps provided by the National Weather Service (NWS), VIP levels, and storm intensity levels are shown in Table 2.

b. The rawinsonde soundings at OKC and SEP at 1200 GMT were used to determine the mean wind structure during the mature stages the storm.

c The records of hourly precipitation from the climatological networks of raingauges were obtained from the National Climatic Data Center. Figures 2 and 3 show the locations of the recording raingauges in Texas and Oklahoma, respectively. These data were plotted and analyzed on the state maps.

d. Sectional surface maps corresponding to the time and location of the MCC were plotted and analyzed. Microbarograph traces and Weather

TABLE 2. Description of Manually Digitized Radar (MDR) Code
(After Foster and Reap 1973).

Code No.	Maximum Observed VIP Values	Coverage In Box	Maximum Rainfall Rate (in./hr.)	Intensity Category
0	No Echoes			
1	1	Any Vip 1	.1	Weak
2	2	≤ 50% of VIP 2	.1- .5	Moderate
3	2	> 50% of VIP 2	.5-1.0	Moderate
4	3	≤ 50% of VIP 3	1.0-2.0	Strong
5	3	> 50% of VIP 3	1.0-2.0	Strong
6	4	≤ 50% of VIP 3 and 4	1.0-2.0	Very Strong
7	4	> 50% of VIP 3 and 4	1.0-2.0	Very Strong
8	5 or 6	≤ 50% of VIP 3,4,5, and 6	2.0	Intense or Extreme
9	5 or 6	> 50% of VIP 3,4,5, and 6	2.0	Intense or Extreme

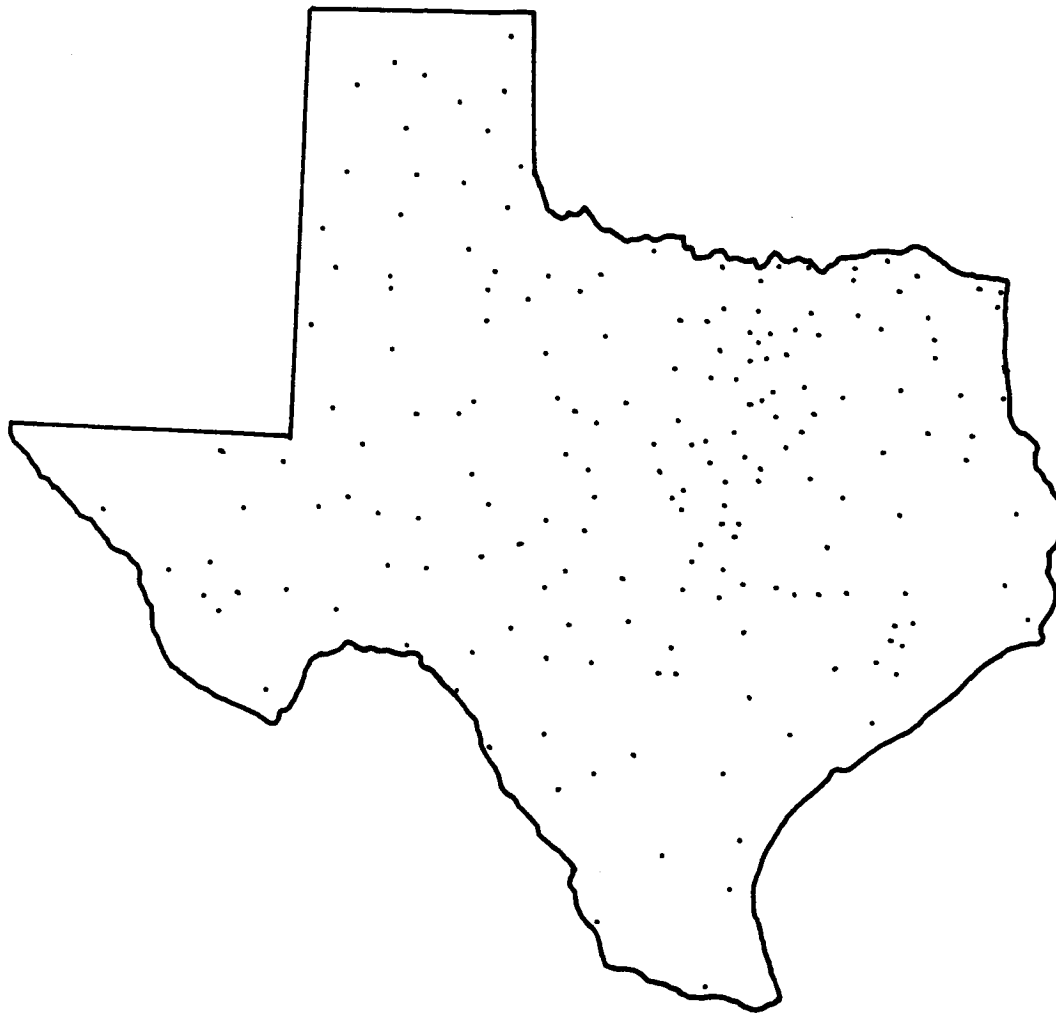


Fig. 2. The climatological network of rain gauges in Texas.



Fig. 3. The climatological network of rain gauges in Oklahoma.

Bureau/Army/Navy (WBAN) records from stations in Oklahoma and northern Texas obtained from the National Climatic Data Center were utilized in this analysis. Gust front position and propagation were more accurately determined with this information and related to radar echo structure and precipitation patterns.

e. The Man-Computer Interactive Data Access System (McIDAS) of the Atmospheric Sciences Division of the Systems Dynamic Laboratory, National Aeronautics and Space Administration Marshall Space Flight Center, was used to obtain hourly, contoured analyses of the cloud top temperature as determined from the GOES IR imagery. This information was combined with the raingauge data.

III. SYNOPTIC CONDITIONS AND STORM HISTORY

The MCC of 27 May 1981 started with isolated thunderstorms over the Texas and Oklahoma panhandles on the afternoon of 26 May. These storms grew in size and intensity and amalgamated. During the evening of the 26th (0100 to 0340 GMT, 27 May) there were two reports of funnel clouds and four reports of tornadoes preceded by golfball-sized hail associated with this storm. These reports came from Briscoe, Motley and Cottle Counties in northwestern Texas very near the Oklahoma border.

Shortly before midnight (0515 GMT, 27 May 1981) the storm system met the criteria for an MCC stated in Table 1. By this time the center of the storm lay roughly on the Red River between OKC and SEP. The maximum extent of the MCC, defined in terms of the area enclosed by the 210 K isotherm depicted in the IR satellite imagery was reached at 1000 GMT on 27 May. Reports of hail came from the northern Texas Archer and Tarrant Counties at 0900 GMT and 1055 GMT, respectively. A windstorm was reported in Fannin County at 0935 GMT.

The termination of the storm as an MCC came at 1400 GMT in the northeastern corner of Texas; however, the system continued to produce precipitation until 1600 GMT.

Figures 4 and 5 show the 70 kPa and 50 kPa analyses for 0000 GMT, 27 May 1981. There is evidence, particularly at 70 kPa of a weak, short-wave trough moving through the long-wave ridge over the area in which the MCC developed. Gurka (1976) found that many summertime, mesoscale systems producing gust fronts observable as arc clouds in

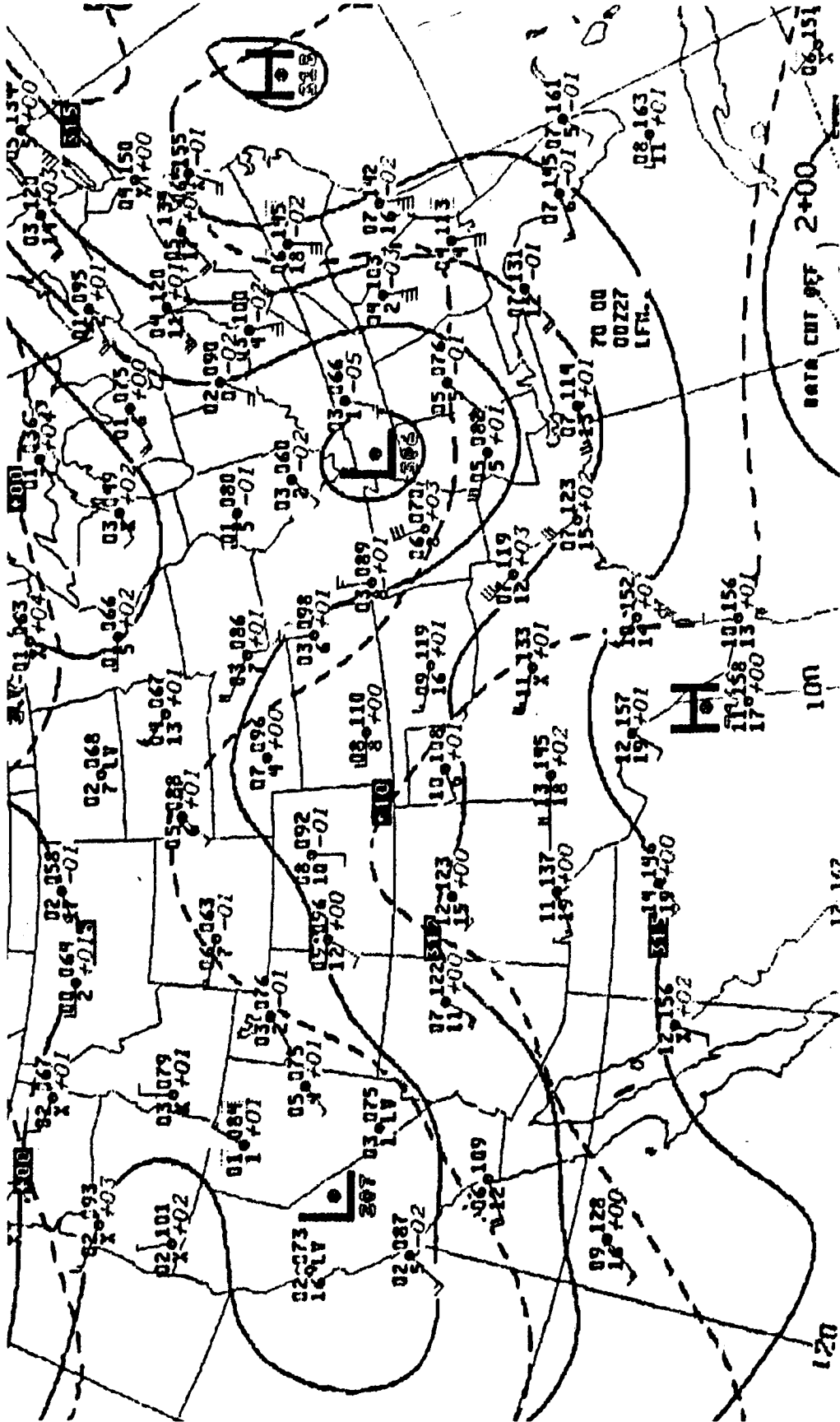


Fig. 4. Synoptic analysis at 70 kPa for 0000 GMT, 27 May 1981. Geopotential height lines are solid, isotherms are dashed.

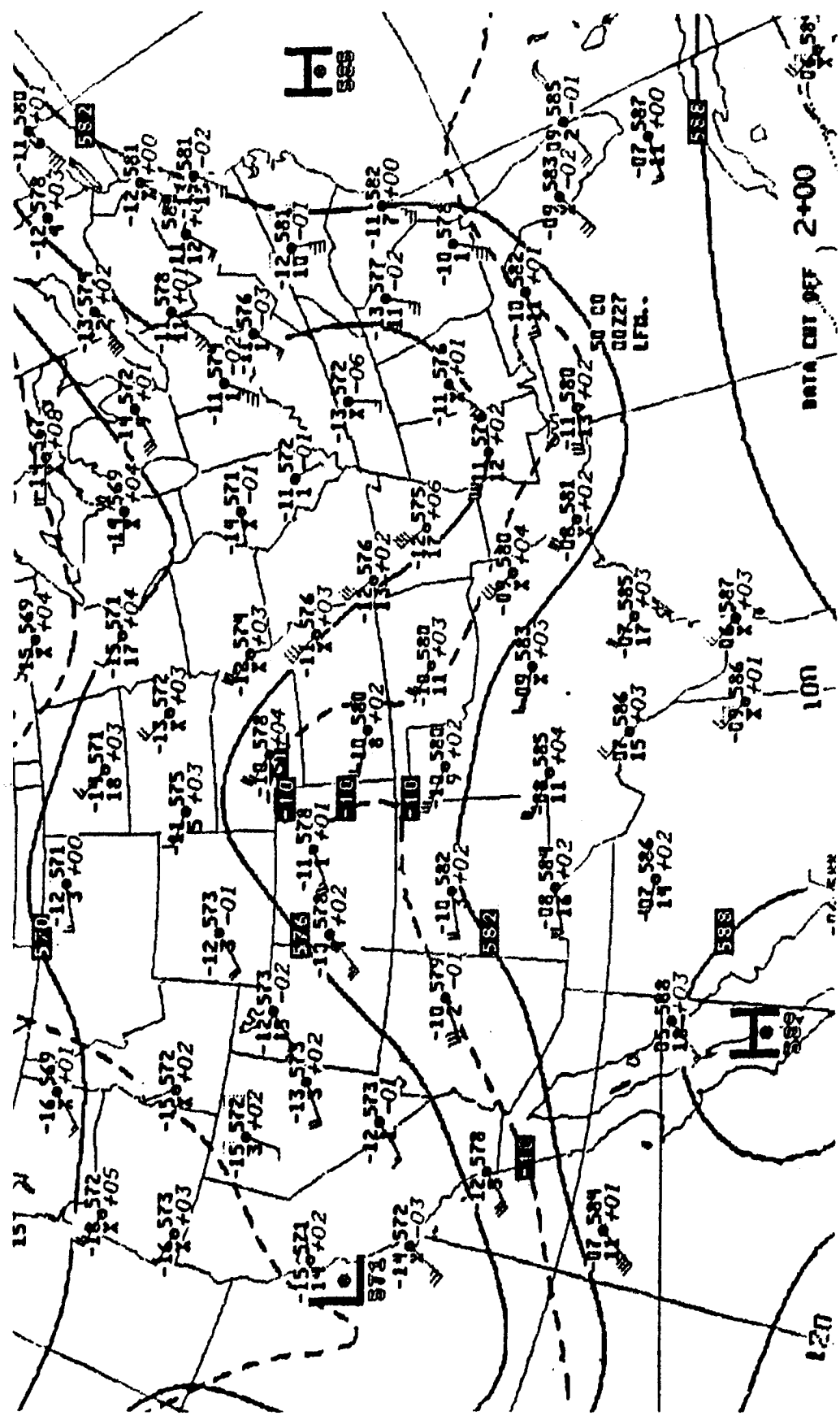


Fig. 5. Synoptic analysis at 50 kPa for 0000 GMT, 27 May 1981. Isolines as described in Fig. 4.

satellite imagery formed in short-wave troughs imbedded in northwesterly flow aloft. The low level warm advection indicated in Fig. 4 may have contributed to the initiation of the MCC. A mesoscale warm pocket is also seen over the area in the 50 kPa analysis.

At 0600 GMT, a mesohigh and strong gust front first appeared in the surface pressure analysis. The gust front, which will be examined later, was located across the Oklahoma/Texas border and was moving southeastward. As it passed Dallas (DAL), TX., a peak wind of 45 kt was one of the indicators that the gust front was quite powerful. Even near termination of the MCC, at 1400 GMT, a strong mesohigh and gust front were still evident in the surface pressure analysis (see Fig 6).

The GOES visible image for 1500 GMT is shown in Fig. 7. Only wide-spread layer-cloud precipitation was occurring at this time. The arc cloud produced by this MCC can be seen in Fig. 7 to be approaching the Gulf Coast of eastern Texas. The arc cloud finally vanished from the satellite images after 1800 GMT.

Other characteristics of this MCC as determined by Welshinger (1985) are shown in Table 3.

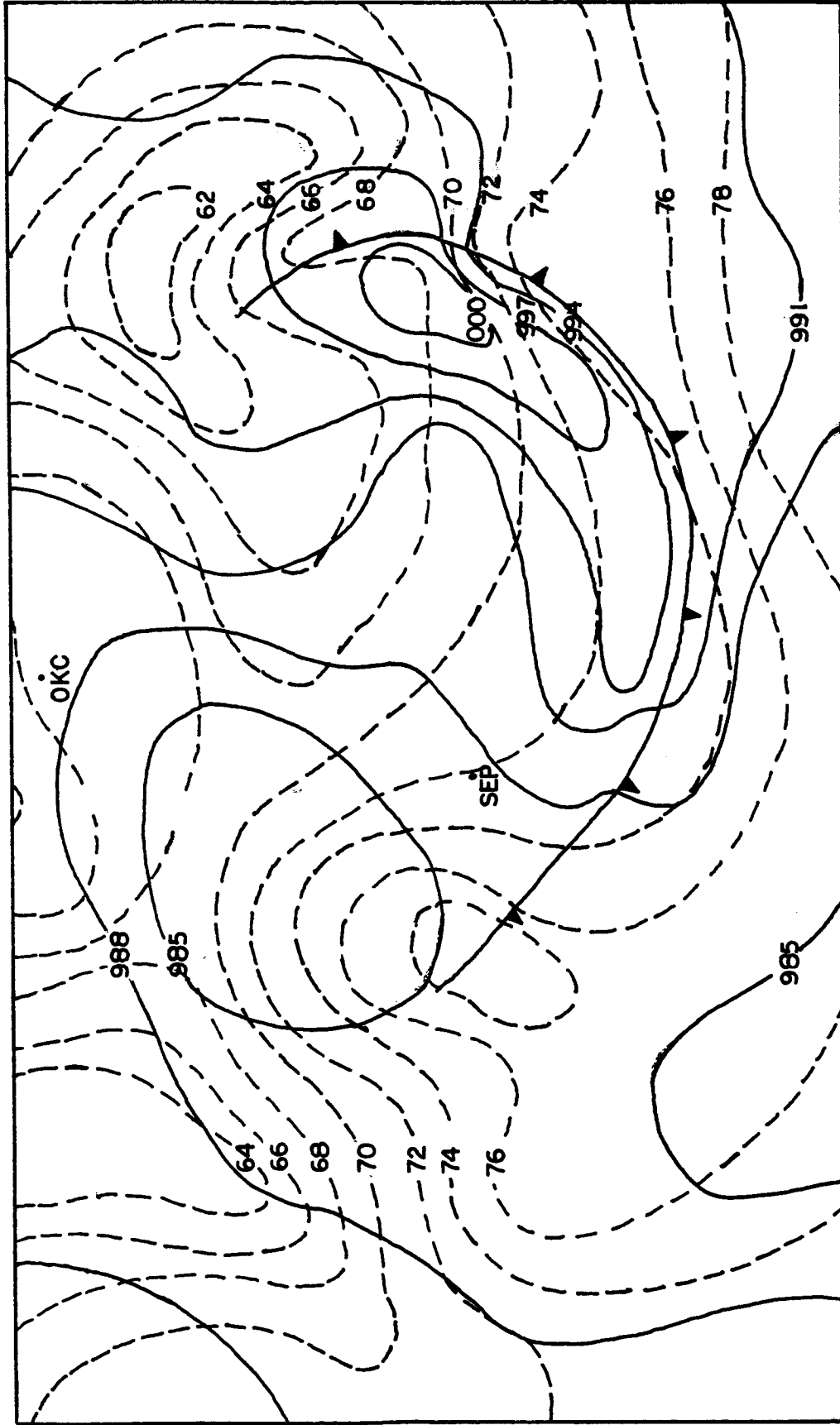


Fig. 6. Surface synoptic analysis at 1400 GMT, 27 May 1981. Pressure contours are altimeter setting values in Hg increments, isotherms are dashed. The gust front is denoted by cold front symbols.

ORIGINAL PAGE IS
OF POOR QUALITY

17

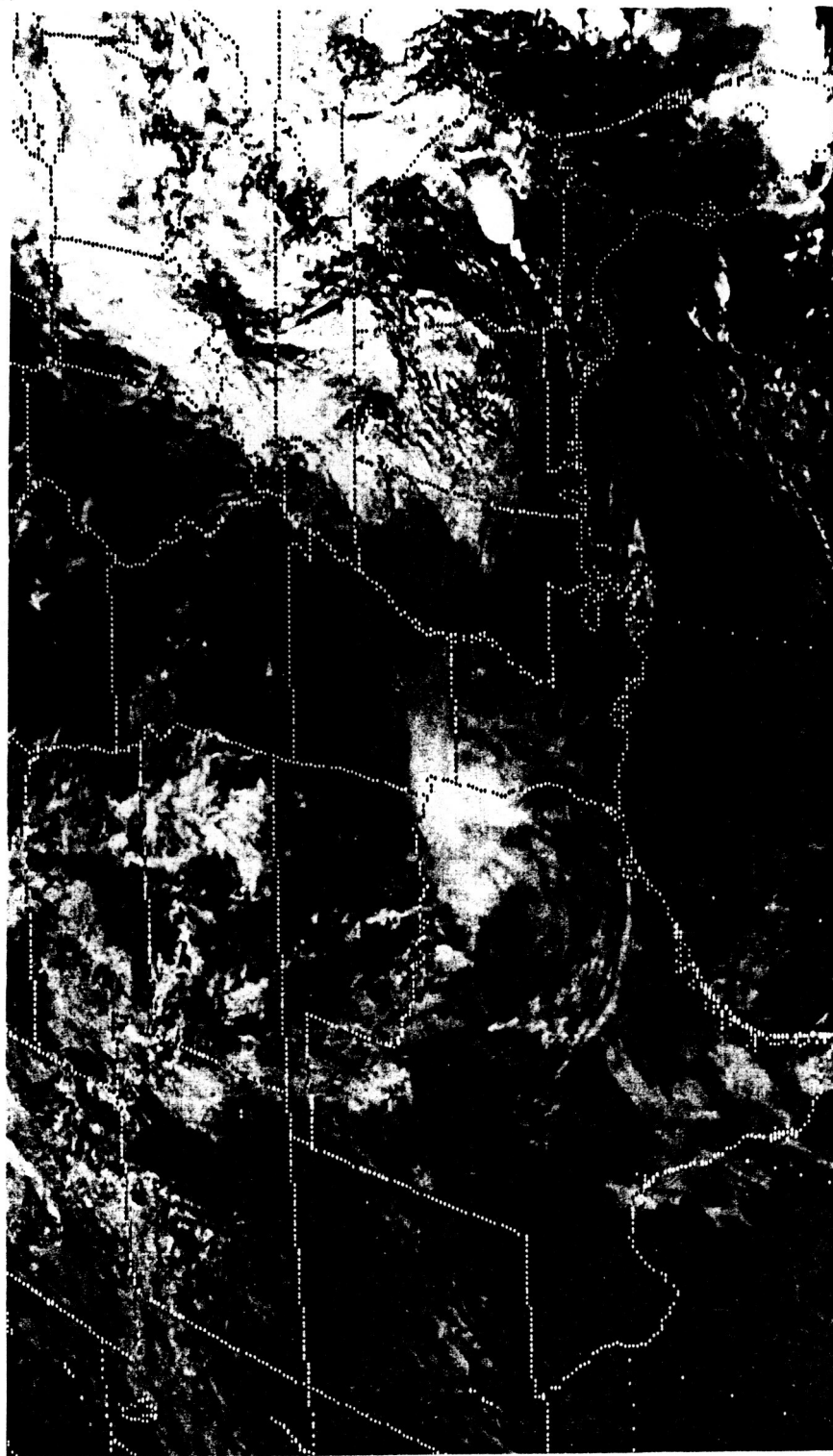


Fig. 7. GOES visible image for 1500 GMT 27 May 1981.

TABLE 3. Characteristics associated with the MCC of 27 May 1981. The maximum thunderstorm heights were determined at approximately 35 min past each hour. Dashes indicate that the parameter was not determined (Welshinger, 1985).

Time (GMT)	Maximum thunderstorm height (x 100 ft)	Maximum surface divergence (x 10 ⁻⁵ s)	Sum of the three largest precipitation rates (in/h)	Maximum point precipitation rate (in/h)	Coldest cloud top temperature (°C)
0400		-	0.60	0.50	-
	520				
0500		-	1.00	0.50	-
	550				
0600		3	1.00	0.70	-
	580				
0700		3	0.73	0.43	-73
	560				
0800		2	1.59	1.30	-68
	520				
0900		2	1.50	0.60	-73
	550				
1000		2	2.70	0.99	-68
	480				
1100		2	2.93	1.13	-68
	470				
1200		2	2.50	0.90	-68
	320				
1300		2	1.61	1.01	-
	250				
1400		3	0.60	0.20	-
	160				
1500		3	0.60	0.20	-
	-				
1600		-	0.10	0.10	-
	-				

IV. STORM MOTION

Figures 8a and b show time sections of the radar echoes at VIP level 1 covering the period from 0000 to 1558 GMT 27 May 1981 at 1 h intervals. This is a composite representation using data obtained simultaneously at OKC and SEP. Due to the elevation angle and the position of the storm between the two radars, data from the southern part and northern part were attenuated for OKC and SEP, respectively. Thus, compositing was necessary in order to get the complete picture. The displacement of the echoes seen in the figure are in part real and in part due to the analysis technique. The radar echoes at 60 min intervals were plotted with respect to the radar station located on the upper sloping line which was oriented from 295 to 115°. After the echoes at a given time were plotted, the station was shifted 20 n mi along this line, and the procedure was then repeated. The station positions and the echoes were labeled with letters related to the time of the observation, as indicated in the figure. Sloping solid straight lines were then drawn connecting individual cells and conglomerations of cells in time. The hatching of the system at 1458 and 1558 GMT was done simply for better identification because it was slow and very small at these times. It must be stated that not all the VIP level 1 echoes that existed at each of the times given in Fig. 8a and b are shown. Only those associated with the main storm area and which existed for at least 1 h were considered.

The time sequence of the echoes reveals interesting features that

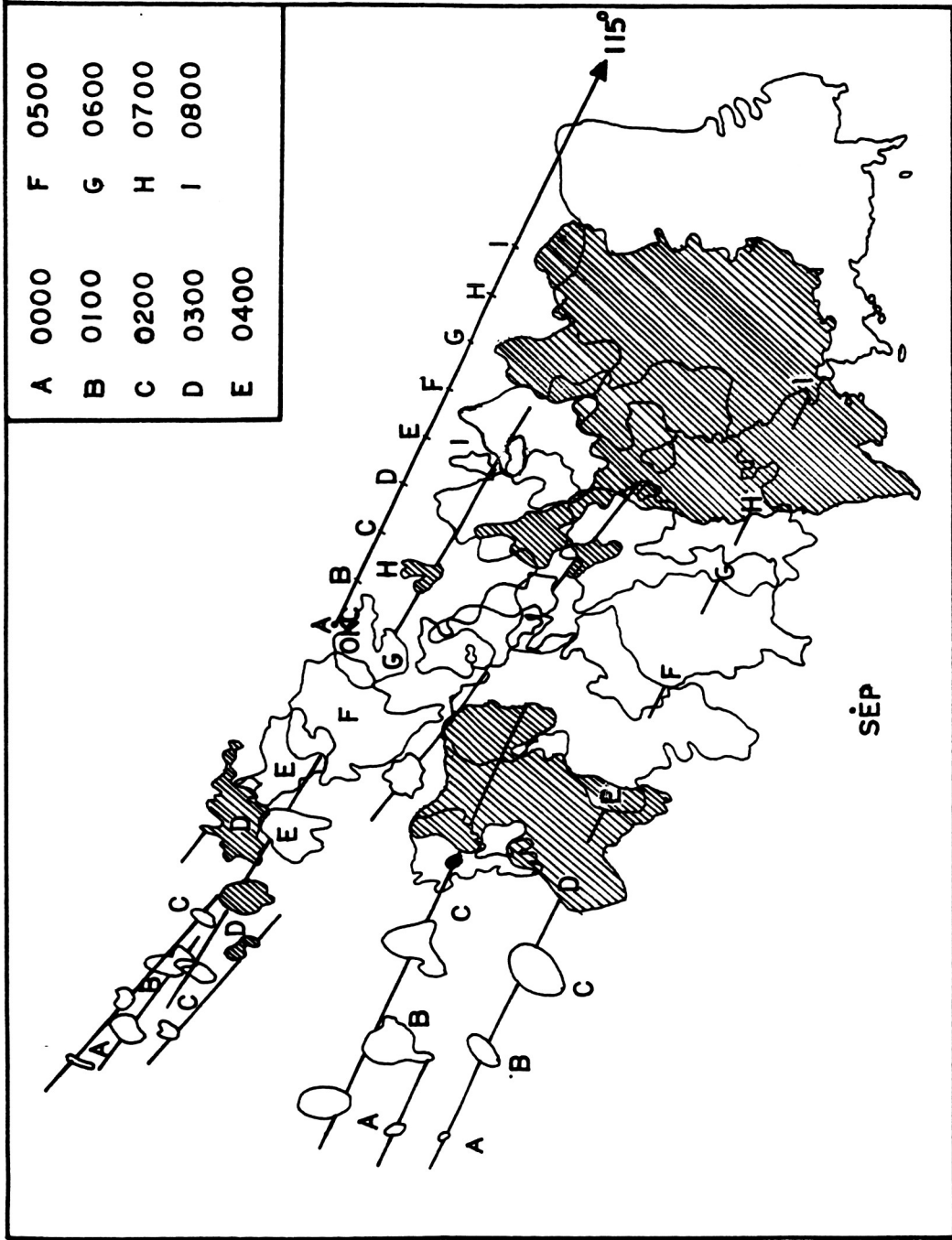


Fig. 8a. VIP level 1 cell outlines at hourly intervals from 0000 to 0800 GMT. Lettered, solid line originating at OKC shows path along which radars were displaced with time for analysis purposes.

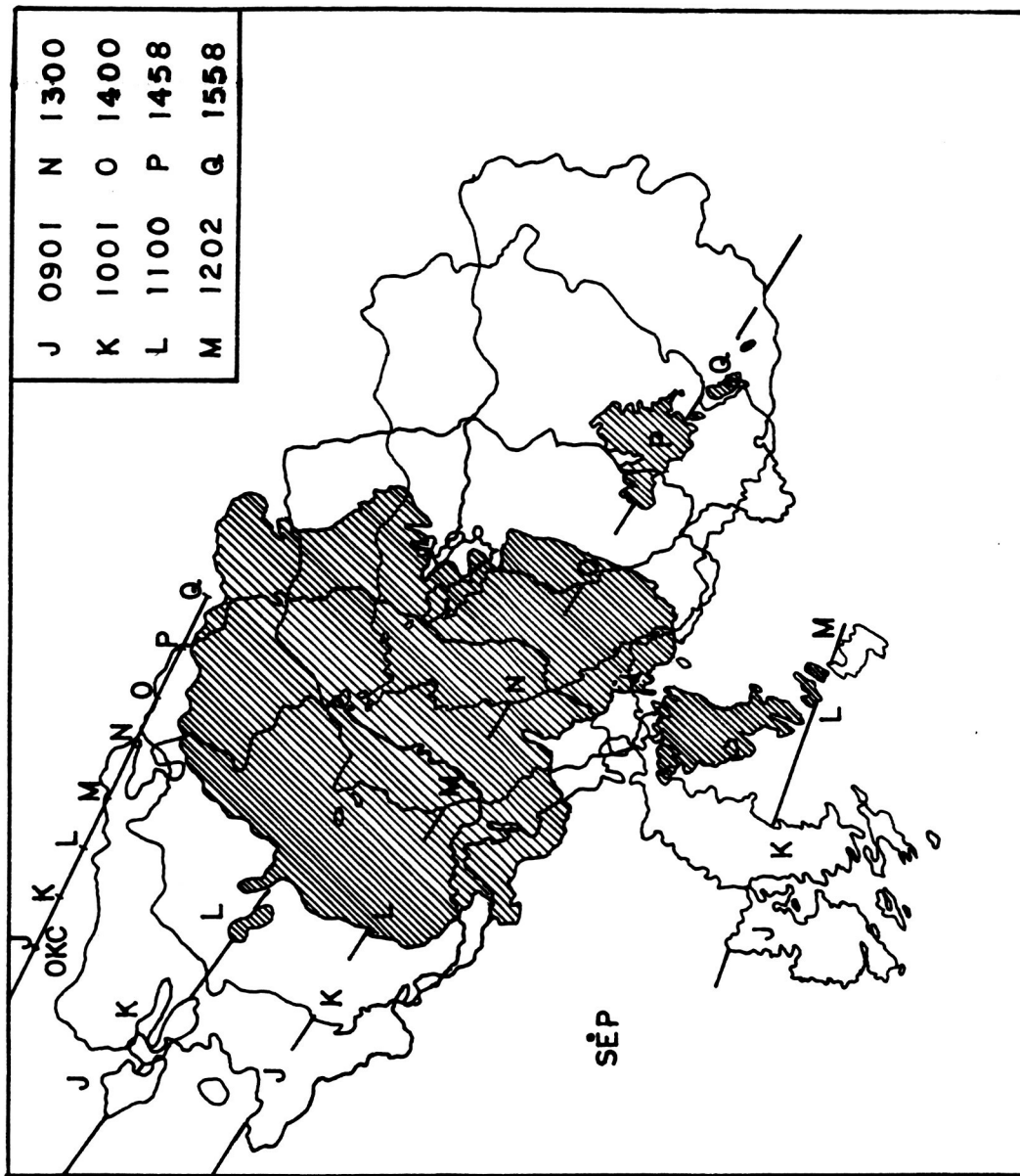


Fig. 8b. As in Fig. 8a except from 0901 to 1558 GMT.

might not be detected with a casual study of the individual echo photographs. It may be noted how the VIP 1 echoes grew in size and merged as the time approached 0515 GMT, the time at which the storm qualified as an MCC. Examination of the figure also indicates the movement of the VIP level 1 echoes varied somewhat from time to time both in direction and speed. However, overall the movement was in the same direction as that chosen for the displacement of the radars, from 295° at a speed of 11 ms^{-1} .

Time sections of the VIP level 3 or more radar reflectivity, covering the period from 0120 to 1240 GMT 27 May 1981 are shown in Fig. 9a and b. The radar echoes at 20 min intervals were plotted by again using a moving coordinate system with a 20 n mi displacement. The station and the echoes were labeled with letters related to the time of the observation. Somewhat erratic cell motion is seen in this figure in that some of these cells moved to left of the storm motion which others moved to the right. Whereas in general, the VIP 3 cells moved at about the same speed as the overall storm (VIP level 1) some cells (hatched in Fig. 9b) which developed starting at 0821 GMT moved at 20 ms^{-1} . When they first appeared, they were located on the west side of the system. By 1240 GMT, they were almost at the middle, southern part of the system.

A careful examination of Fig. 9 also reveals that the appearance of new cells, or vanishing of old cells, did not take place in a consistent fashion. For example, new cells appeared on the north side of the developing system at 0341 GMT, 0400 GMT and 0440 GMT. Some of

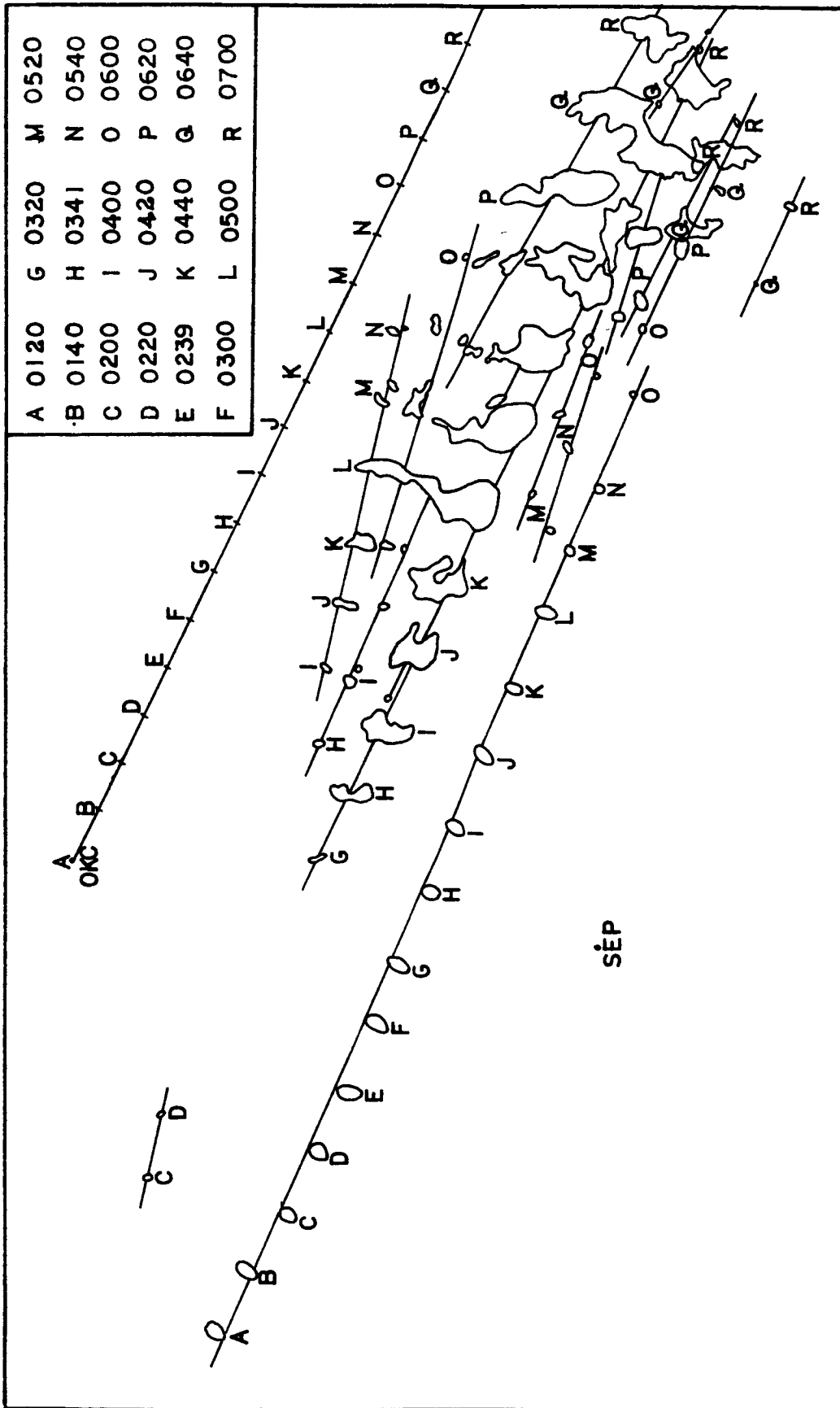


Fig. 9a. VIP level 3 cell outlines at 20 min intervals from 0120 to 0700 GMT. Solid line through OKC shows displacement path of radars.

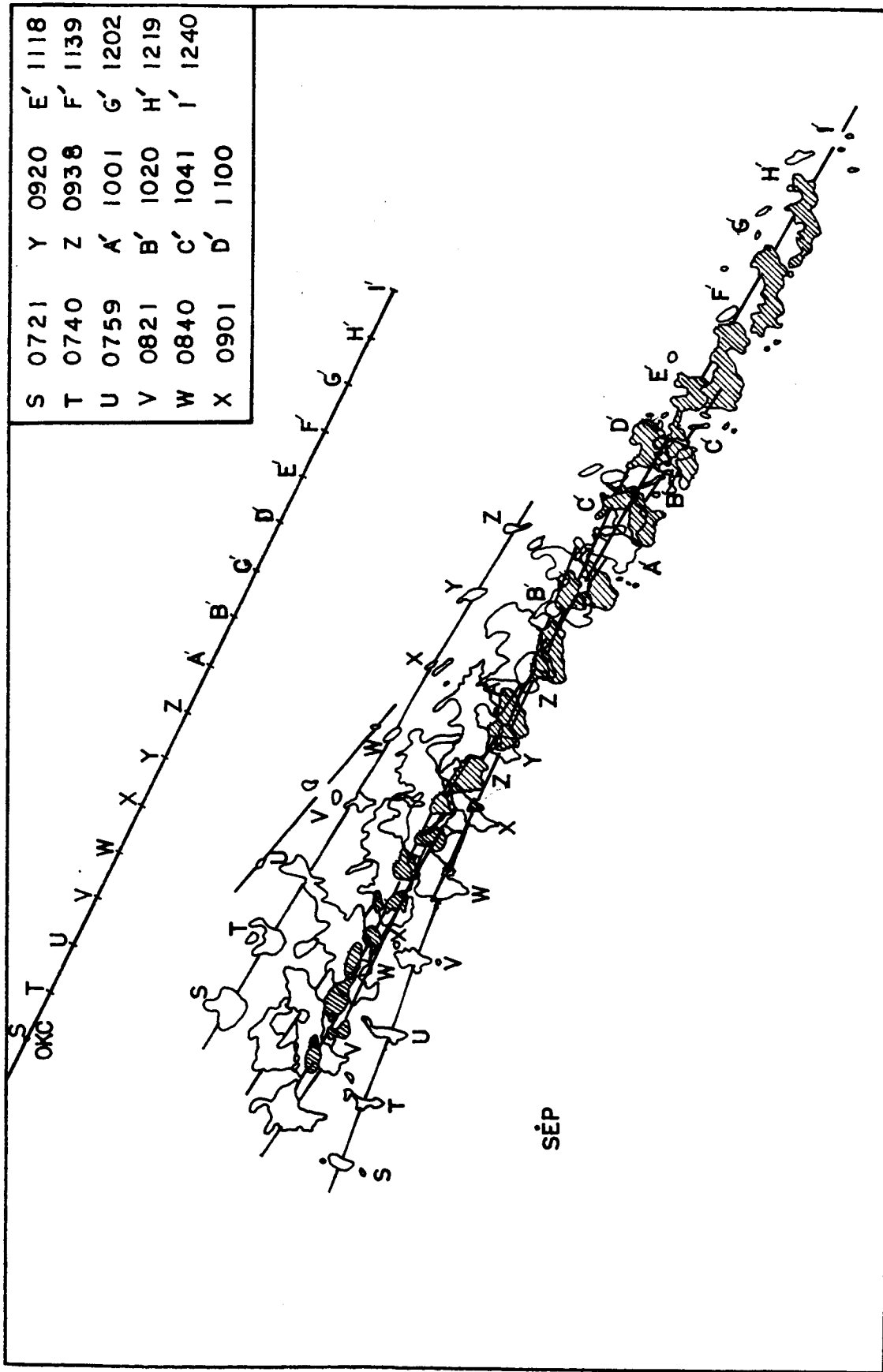


Fig 9b. As in Fig. 9a except from 0721 to 1240 GMT.

these eventually dissipated. Likewise, new cells appeared on the south side of the system at 0520 GMT, 0600 GMT and 0620 GMT. Again, some of these cells dissipated. New cell development also took place to the rear of the primary convective line, starting around 0821 GMT. Thus a consistent pattern of cell development on one side of the storm and dissipation on the other side, such as found by Marwitz (1972) did not occur in this case.

The mean wind flow in the vicinity of storm was determined from 1200 GMT rawinsonde measurements at OKC and SEP. This observation time was chosen because it was closest to the time of maximum extent of the MCC, 1000 GMT.

Figure 10 is a hodograph plot of the winds at OKC and SEP at the 85, 70, 50, 30 and 20 kPa levels. The average propagation vector of the storm (and the VIP level 3 cells), from 295 at 11 ms⁻¹, also is indicated. This speed is moderate compared with some reported in the literature (Maddox and Howard, 1983).

The mean cloud -layer wind vector and mass-weighted mean wind vector also are shown in Fig. 10. The mean cloud-layer wind was calculated by first determining the mean vector wind for each station over the layer from 85 to 20 kPa, and then averaging the resulting two vectors. The mass-weighted wind was calculated in the same way but using the relationship

$$V_m = \frac{\sum_{i=1}^N \rho_i v_i}{\sum_{i=1}^N \rho_i}$$

where ρ is density and the summations extended from 85 to 20 kPa. It is

- 0. Surface
- 1. 850 mb
- 2. 700 mb
- 3. 500 mb
- 4. 300 mb
- 5. 200 mb

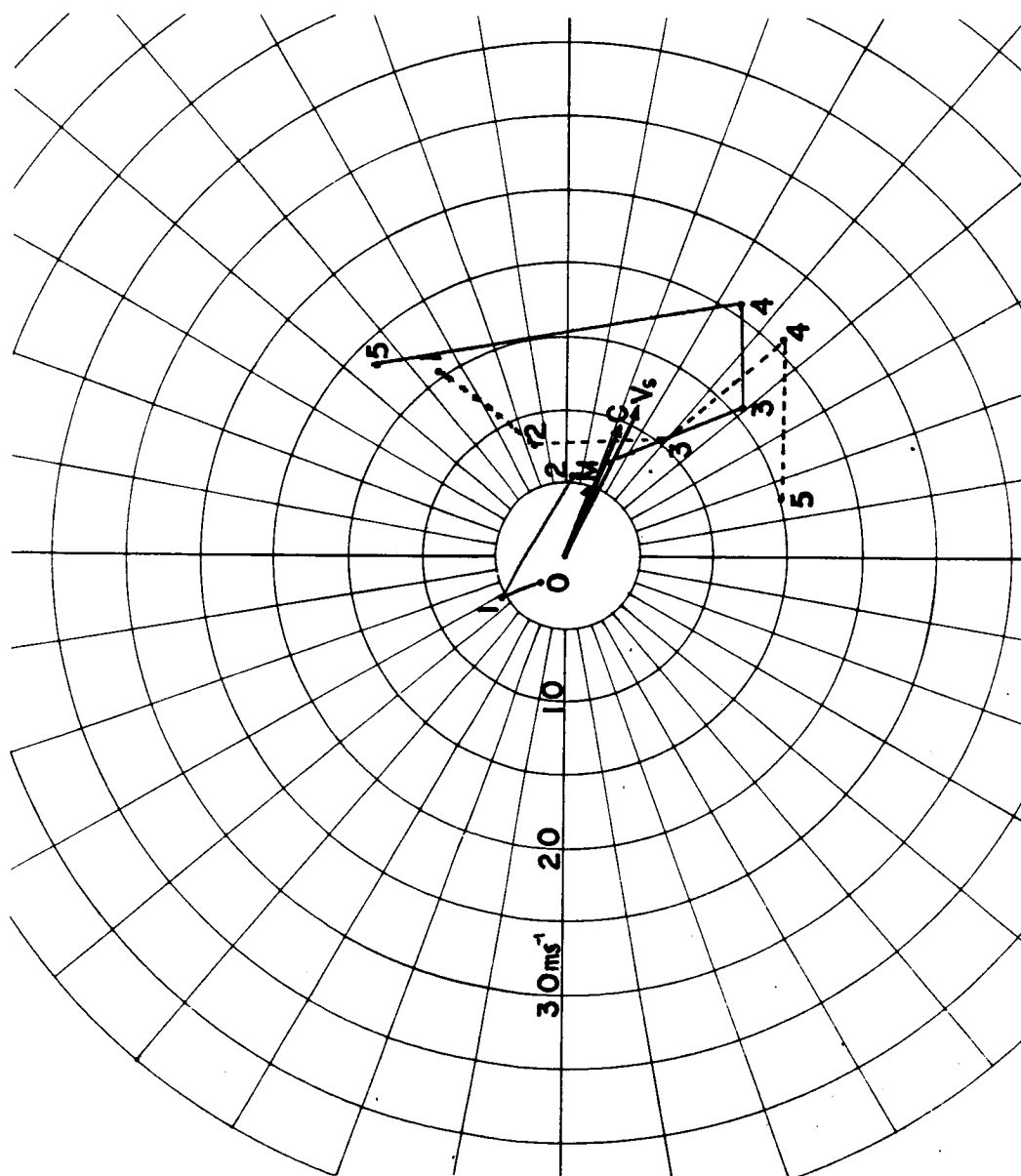


Fig. 10. Hodographs at 1200 GMT for OKC (solid) and SEP (dashed). Winds are shown for the surface and mandatory pressure levels from 85 to 20 kPa. Storm motion V_s , the cloud-layer wind C and the mass-weighted vector M are plotted.

seen that the mass-weighted vector has the same direction as the mean cloud-layer wind vector but is smaller in magnitude. On the other hand, the mean cloud layer wind matches very well with the storm vector, allowing for errors in wind observations and determination of echo displacements. Zehr and Purdom (1982) found that the direction of the mean cloud layer wind is usually very similar to the 50 kPa wind. It can be seen that this match is close for SEP but not as good at OKC. Likewise, the 1 km-50 kPa shear vector found as an indicator of the MCC motion by McAnelly and Cotton (1986) does not work well for this MCC.

The observed winds at OKC and SEP in comparison with the storm motion show that the relative motion of the air at and below 70 kPa was into the storm from the front and right flanks; this continuous supply of low-level moist air no doubt contributed to the maintenance of the storm. At and above 50 kPa, dryer environmental air was entering the system from the left and rear flanks.

Figure 11 again shows the VIP level 1 echoes; however, this representation differs from that shown in Fig. 8a and b in several ways. First, in this representation, the echoes have not been translated relative to the radar sites, thus their true positions as a function of time relative to OKC and SEP are shown. Secondly, the letters in Fig. 11 show the instantaneous position of the echo centers; therefore, the confusing overlapping of echo areas appearing in Fig. 8a and b is eliminated. Finally, Fig. 11 shows all VIP level 1 echoes, regardless of lifetime or position, at the given times. Thus, echoes outside the main storm area are shown, e. g. note the echoes at 1202

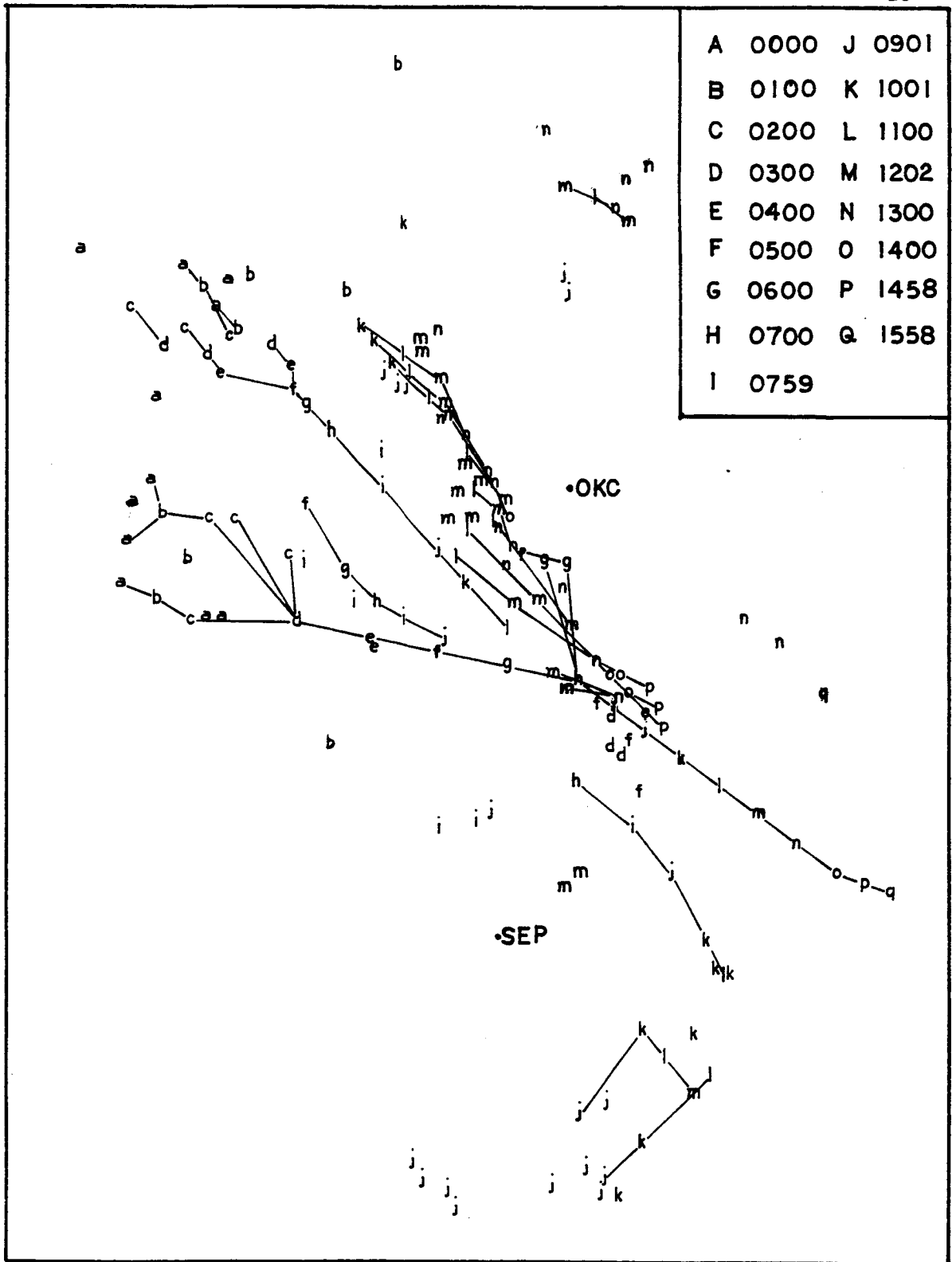


Fig. 11. VIP level 1 cell centroid positions at hourly intervals from 0000 to 1558 GMT. Variations in propagation direction through the lifetime of the storm are evident.

GMT appearing to the north and west of OKC.

This figure shows somewhat more clearly how the tracks of the echoes varied in direction through the lifetime of the storm. About 0901 GMT, new VIP level 1 echoes developed to the south of the main storm area and moved toward the northeast. In all likelihood, these echoes were related to warmer clouds and their motion was a result of the low-level flow.

V. NEW CELL DEVELOPMENT

One objective of the study was to examine how new cells (VIP level 3 or more) developed in relation to the gust front of the system as a whole. Figure 12 shows the trajectories of selected VIP level 3 cell centers in conjunction with the positions of the gust front in time. Many of the cells shown in Fig. 9 are not included here. The gust front positions were determined from the combination of WBAN logs and microbarograph traces from selected stations coupled with sectional surface observations.

The simultaneous positions of the cells and the gust front in time are labeled with letters at approximately 1 h intervals, as in previous figures. The gust front was not identifiable until after the storm had become an MCC. Thereafter, it was found on the eastern, southern, and western extremities of the VIP level 1 echo field- more will be said about this relationship later. Figure 12 again shows the great variability in the trajectories of the cells. Furthermore, it shows that new cells developed along and behind the gust front, and either dissipated quickly or translated toward the southeast along with the gust front for several hours before dissipating. In some instances, merging of cells occurred.

One interesting phenomenon which can be seen to some extent in Fig. 12 is the tendency of the region of greatest reflectivity to appear as a line oriented in a somewhat south to north direction in the early life of the MCC. Note the cells labeled A at 0600 GMT. In this case, as

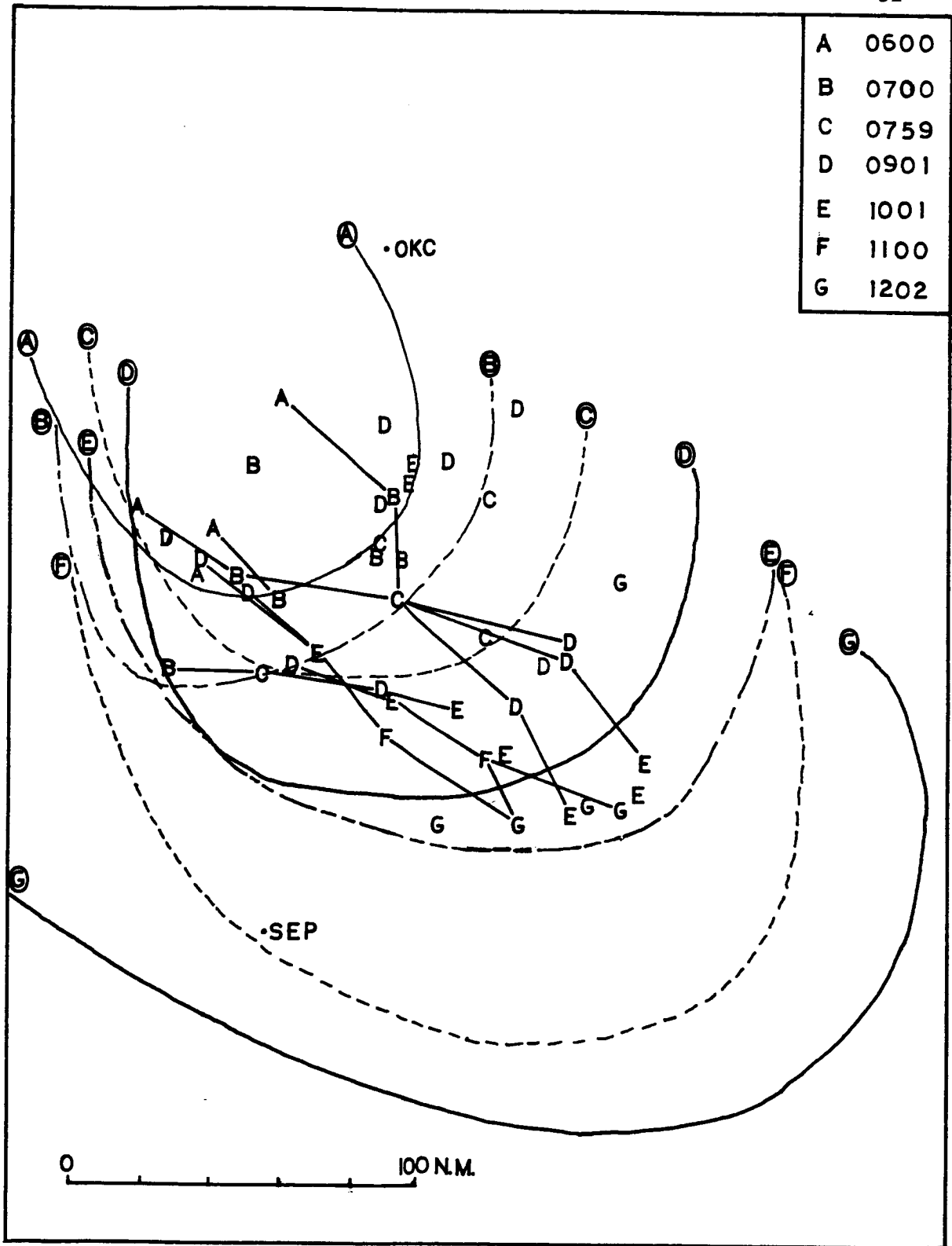


Fig. 12. Gust front and level 3 cell positions at hourly intervals.

time went on, older cells progressed southeastward while new cells developed behind the less-mobile, western side of the gust front- see the cells labeled D at 0901 GMT. Consequently, the maximum reflectivity became oriented along a more west-east line. This phenomenon also has been observed by Howard and Maddox (1983) and Bartels and Rockwood (1983). In the first case, the western end of the line eventually developed into a second MCC. After the time of the maximum extent of the MCC at 1000 GMT, it is seen in Fig. 12 that the gust front accelerated and no new cell development occurred after 1202 GMT.

Although it cannot be ascertained with certainty with these observations, it appears likely that the gust front plays a significant role in the development of new VIP level 3 (or more) cells, as suggested by Maddox (1980b). At some time it moves outward so far from the primary convective activity that the associated low-level horizontal convergence no longer can maintain the storm.

VI. RADAR DATA DETAILS

The echoes seen in Fig. 13 at 1 h intervals from 0100 to 1558 GMT illustrate the important evolutionary features of the MCC. Outer solid lines denote the VIP level 1 systems, and hatched regions denote the cells with VIP level 3 or more reflectivity. The blackened region at 0200 GMT and later times denotes no radar echo as a consequence of attenuation. At 0300 GMT the precipitation amount was 0.3 in at McLean, TX. These precipitation values represent accumulated amounts over the previous hour from the climatological networks of raingauges. The dot in the figure shows both the location of the precipitation and the decimal point. The storm was growing and at 0400 GMT moderate rainfall had occurred at Altus, OK. Over the hour from 0300 to 0400 GMT this incipient MCC produced funnel clouds and tornadoes in Texas.

The storm intensified rapidly and met MCC criteria by 0515 GMT. The expansion in area of the system is apparent from comparison of Figs. 13 e and f. Moderate rainfall occurred during the initiation time. The northeast to southwest oriented line of cells (VIP level 3 or more reflectivity) continued to move eastward for several hours (Fig. 13d-g), with the northern cells moving somewhat faster on convergent tracks. About three quarters of an hour after the initiation of the MCC, a mesohigh and gust front formed across the Oklahoma/Texas border and subsequently moved southeastward. As the MCC intensified, scattered rainfall occurred, and moderate to heavy rainfall was reported in the vicinity of the VIP level 3 cells. During the merging of the discrete

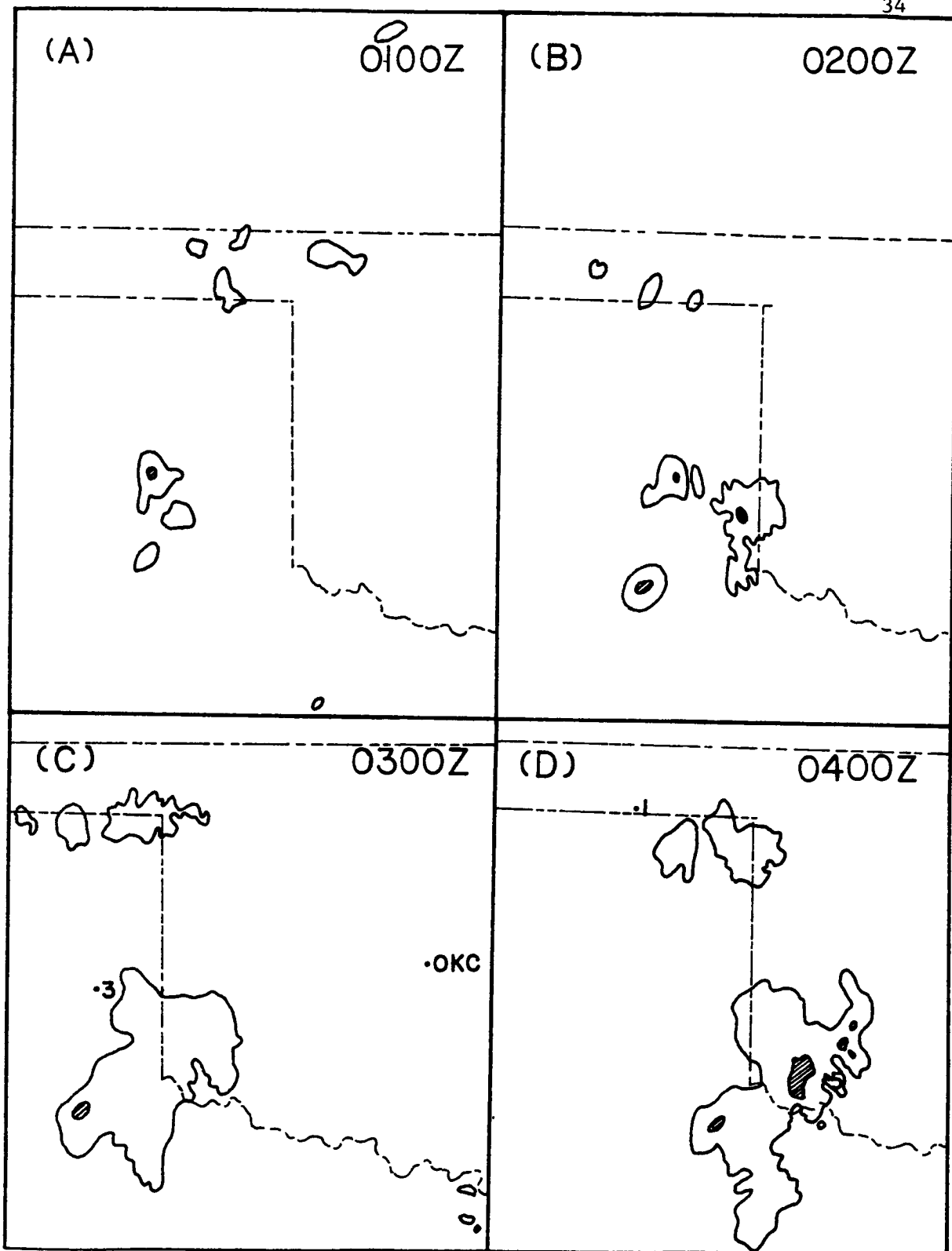


Fig. 13. Combined level 1 and level 3 radar echoes at hourly intervals from 0100 to 1558 GMT. Outer contours represent VIP level 1 echoes; level 3 echoes are hatched. One-hour accumulated rainfall amounts from recording raingages are shown. Starting with 0600 GMT, the gust front is denoted by cold front symbols. Blackened areas indicate radar attenuation.

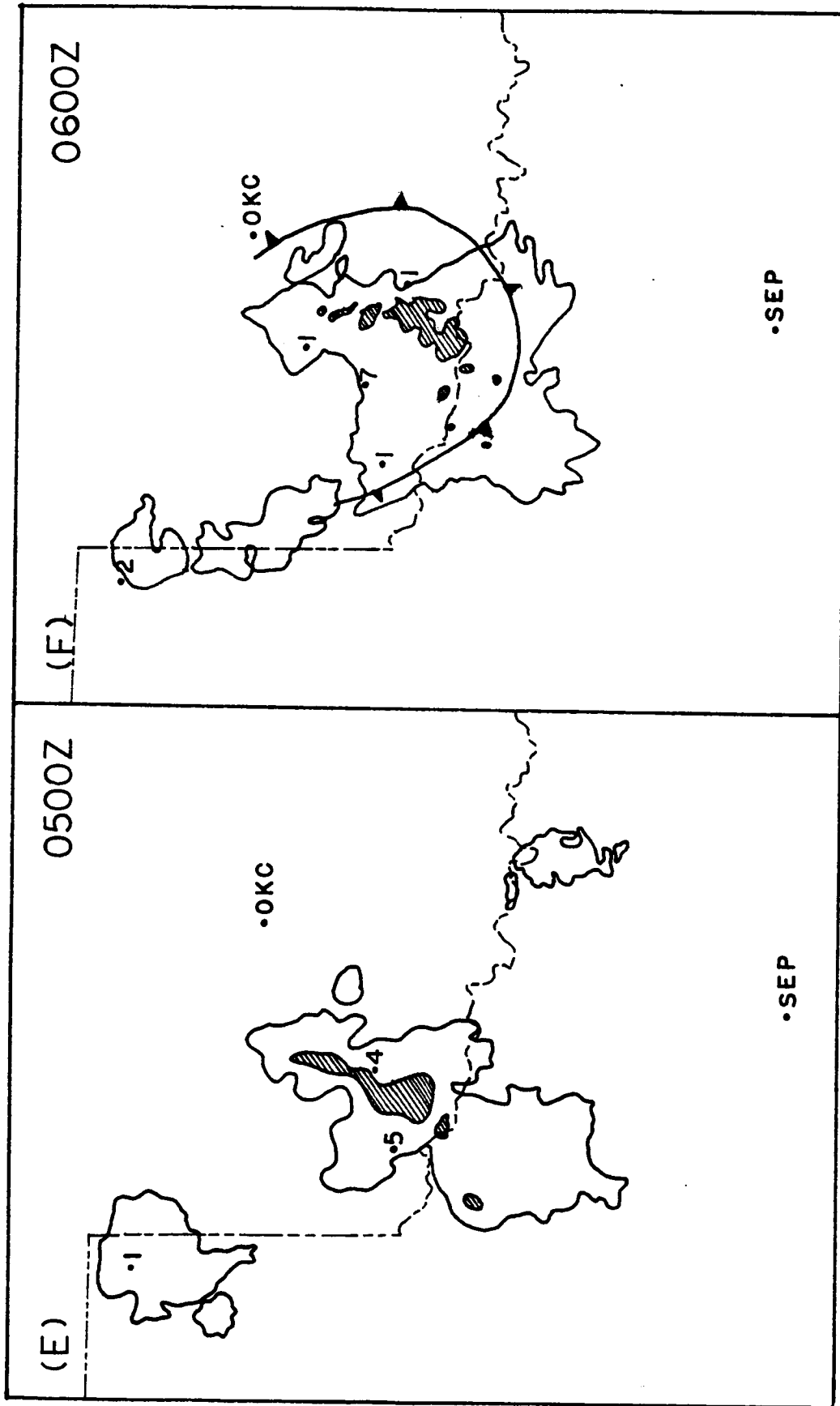


Fig. 1.3. (Continued)

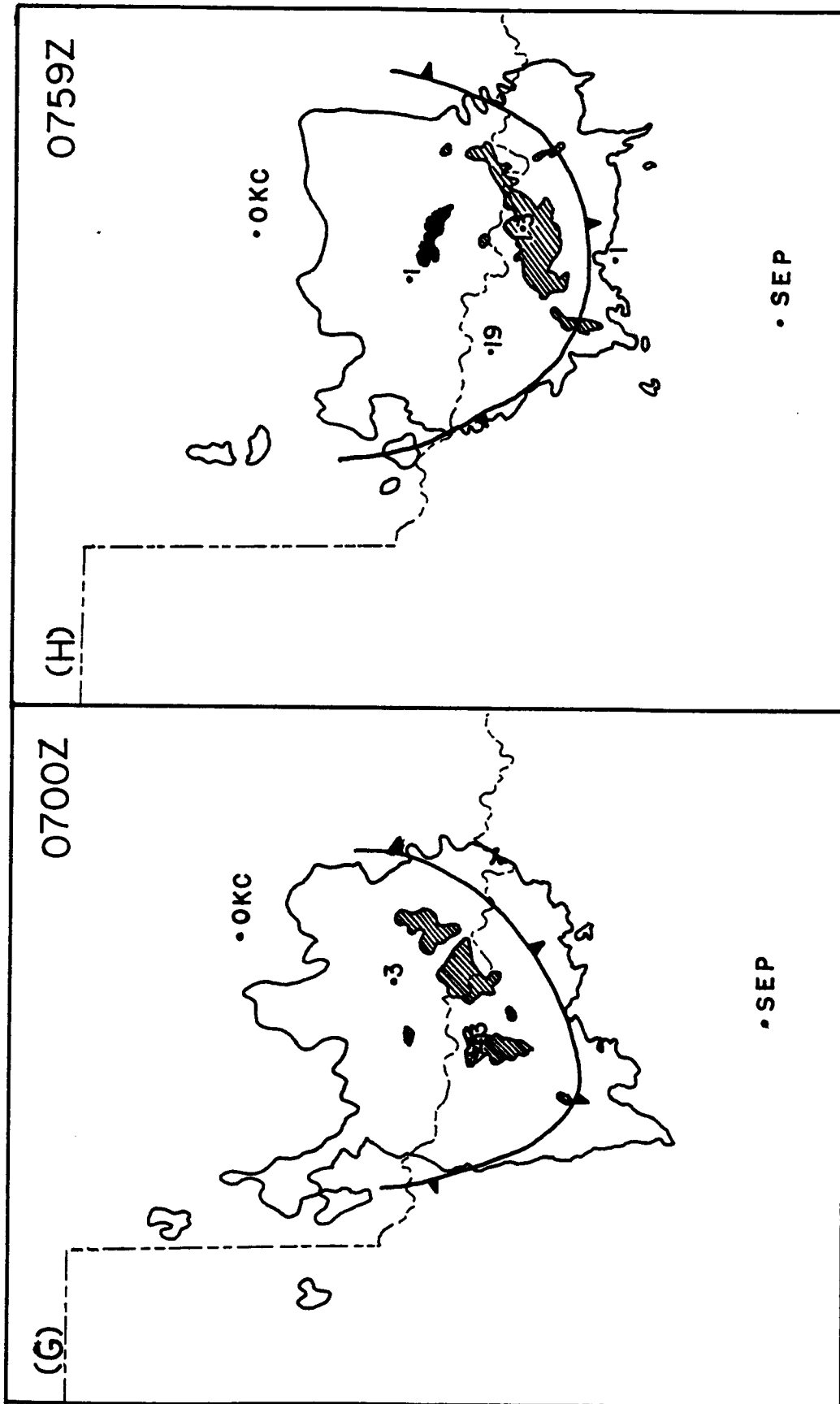


Fig. 13. (Continued)

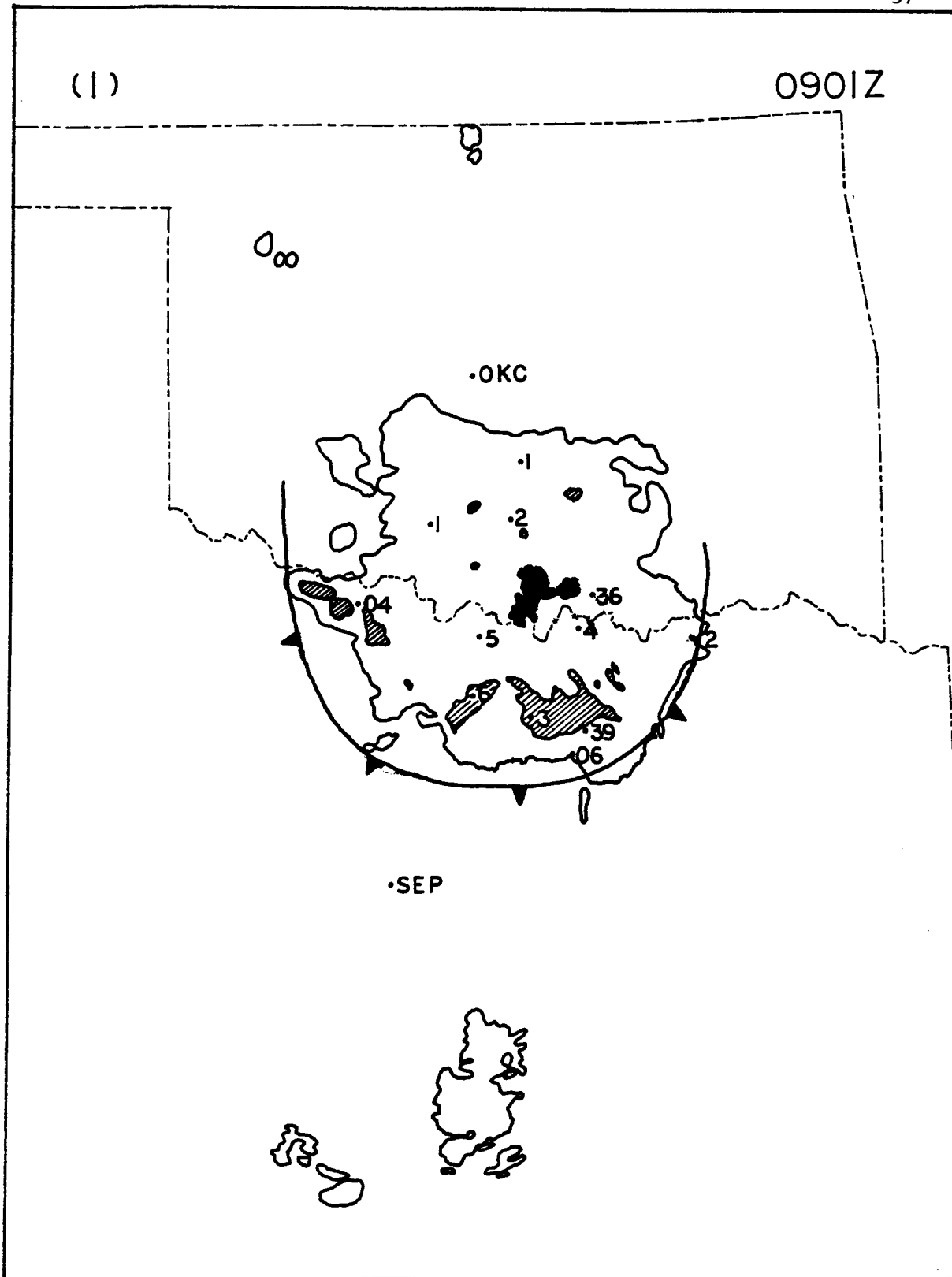


Fig. 13. (Continued)

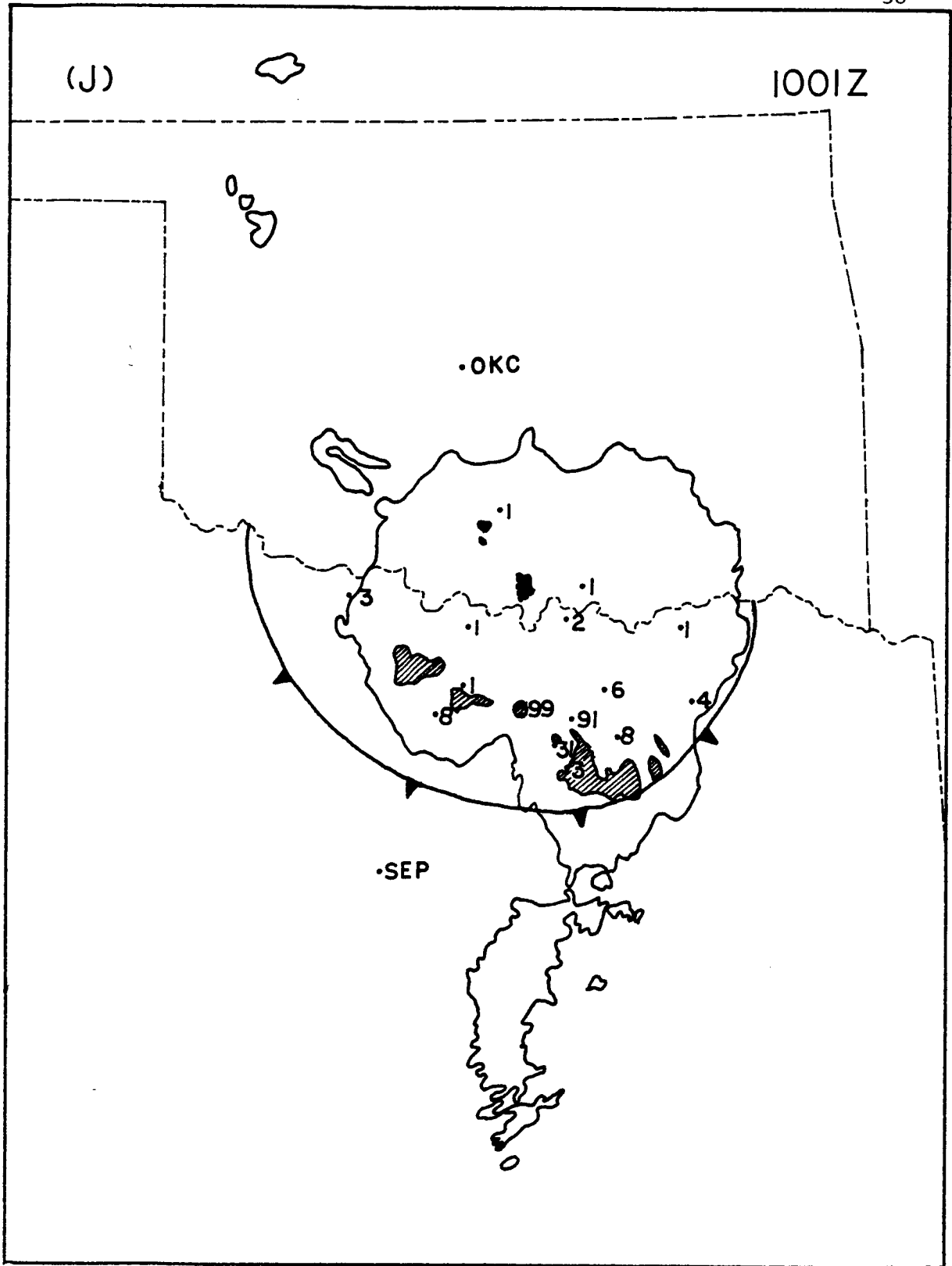


Fig. 13. (Continued)

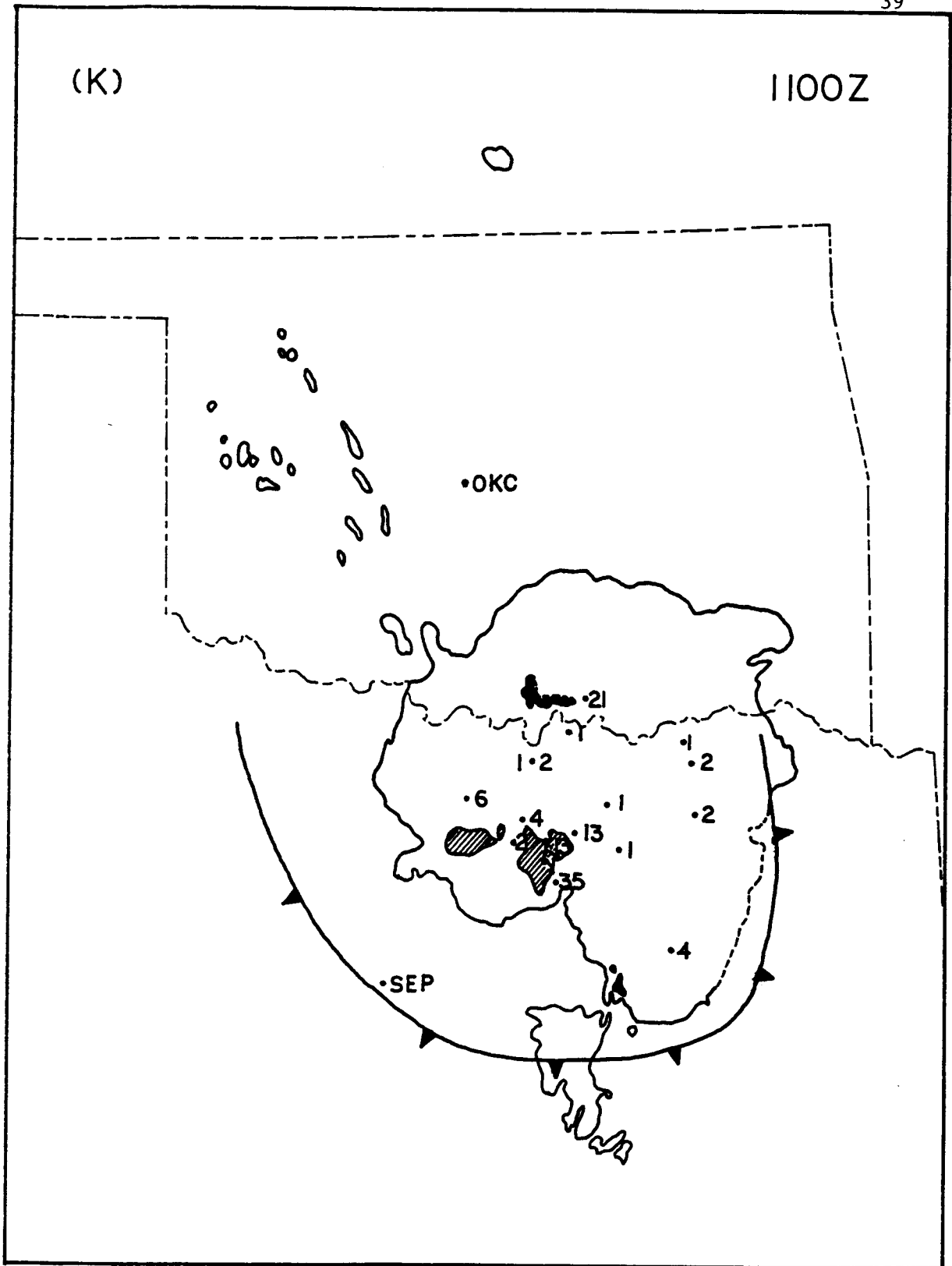


Fig. 13. (Continued)

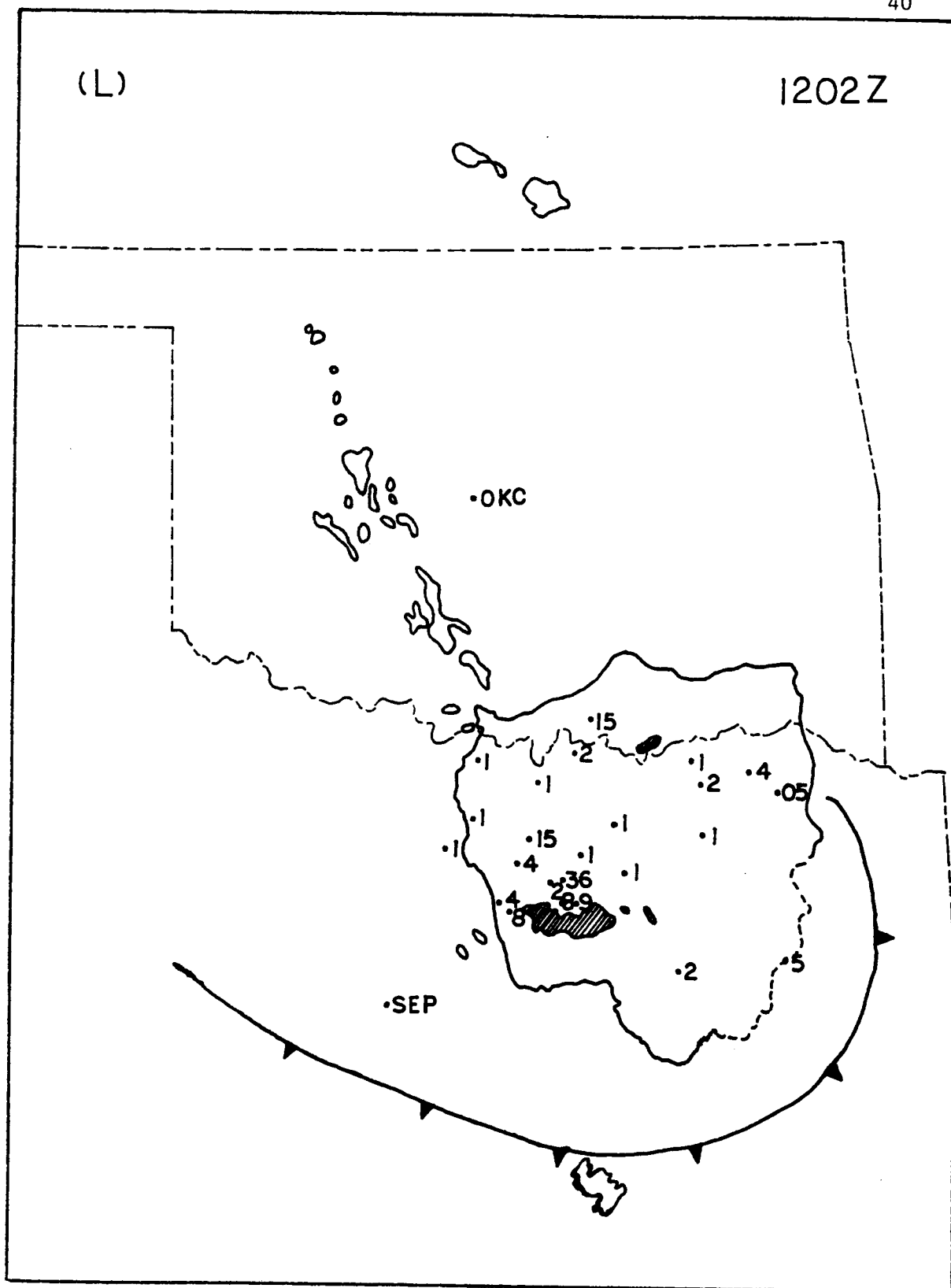


Fig. 13. (continued)

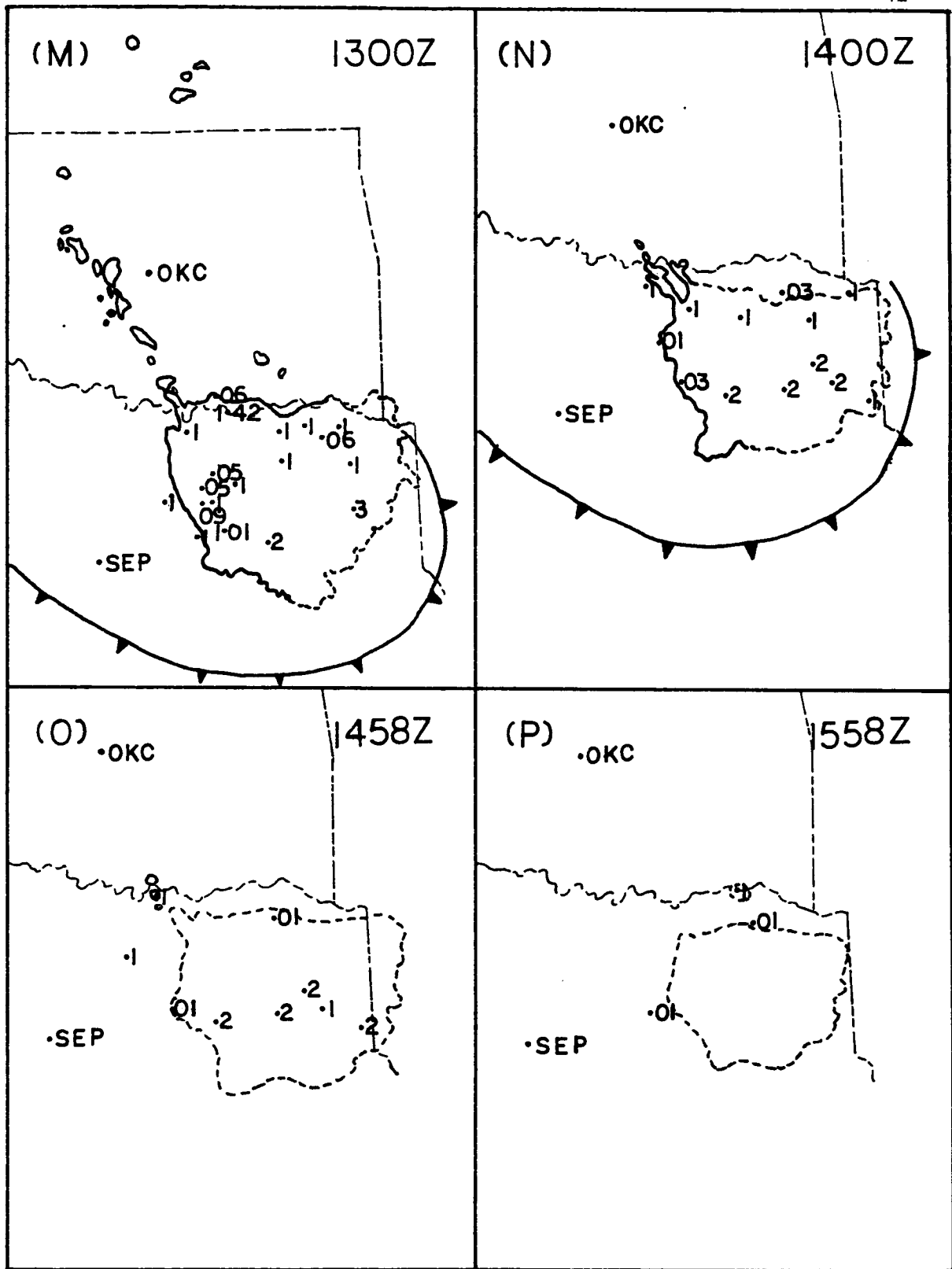


Fig. 13. (Continued)

cells into a larger area of widespread intense reflectivity at Gordonville, TX., rainfall of 1.3 in was recorded (see Fig. 13h). In Figs. 13f-i new cells can be seen to have developed right along the gust front. The MCC rapidly developed after 0800 GMT and the clockwise rotation of the axis of maximum reflectivity, which was mentioned before, can be seen to have taken place between 0600 and 0901 GMT. Very high reflectivity (more than VIP level 3) was observed at 0901 GMT. The strength of the gust front at the same time was revealed by the strong and gusty winds which it produced. At 0935 GMT, as the gust front passed Dallas, TX. a peak wind of 45 kt was recorded.

Figure 13j shows the system at the time of maximum intensity. Although the system was fully developed, the reflectivity was somewhat weaker and there were fewer VIP level 3 cells. Nevertheless, heavy rainfall occurred in the vicinity of the VIP level 3 cells. After 1100 GMT, the gust front moved away from the storm and the system began to dissipate. The dashed boundary on the east side of the wide-spread area of rain in Fig. 13l had to be estimated because of attenuation of both radar beams.

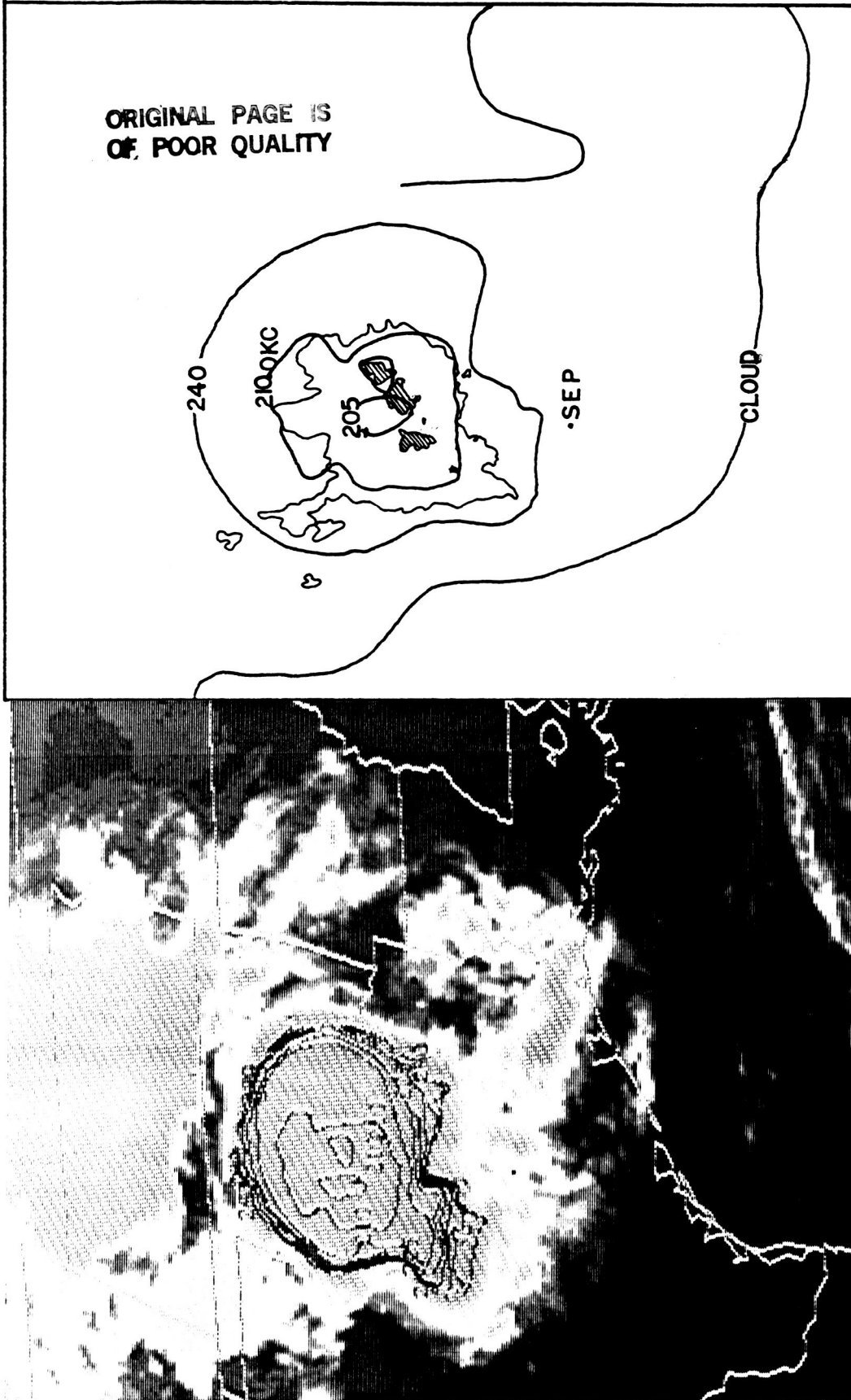
By 1300 GMT, all VIP level 3 or more cells had vanished; however, during the previous hour strong rainfall had occurred in the amount of 1.01 in at Ferris, TX, and 1.42 in at Denison Dam, TX. These heavy rainfalls were produced by the fading VIP level 3 cells at 1202 GMT. Near the termination time of the system, rainfall was wide-spread and light rainfall continued for another 2 h thereafter.

VII. COMBINATION OF SATELLITE IMAGERY AND RADAR OBSERVATION

Figures 14 through 18 represent comparisons of satellite imagery with VIP level 1 and 3 radar patterns at a number of times through the lifetime of the storm of 27 May 1981. Included in these figures are contours of cloud-top temperatures determined from the GOES IR imagery through the use of the McIDAS system at the Marshall Space Flight Center. The reader may wish to compare these figures with Figs. 13g-13l which show the same radar patterns coupled with the gust front positions.

Figure 14 shows the situation at 0700 GMT. On the right-hand side of the figure, the outer line shows the overall cloud shape, as provided by the satellite image on the left-hand side of the figure. The inner, thicker lines depict the cloud top equivalent blackbody temperatures of 240°, 210°, and 205°K.

The satellite image displays a large, nearly circular shield of cloud, as required in Maddox's definition (1980) for an MCC, with coldest tops occurring over the west central portion of the system (compare with Fig. 13g). The radar depiction on the right-hand side of Fig. 14 indicates that the VIP level 1 rainfall at this time was fairly well contained within the 210°K or -63°C isotherm of the storm canopy. About half of the VIP level 3 echo fell within the 205°K isotherm. Also, further comparison with Fig. 13g shows that the gust front position in Fig. 13g falls between the 210 and 240°K isotherms shown in Fig. 14. Gurka (1976) found that the gust front generally is



ORIGINAL PAGE IS
OF POOR QUALITY

Fig. 14. Simultaneous views of satellite imagery and radar echoes at 0700 GMT. On the left-hand side is the GOES IR image with superimposed equivalent blackbody temperature field (K). On the right the outermost line is the boundary of the cloud shield. Inner lines show IR temperature field superimposed on the radar echo pattern.

located very close to the strongest gradient in IR temperature on the eastern and southern sides of a mesoscale storm

Figures 15 through 18 in general show the same features as noted in Fig. 14. Figures 15 and 16 show good agreement between the 210°K isotherm, the boundary of the VIP level 1 reflectivity region, and the position of the gust front. There is some tendency for the VIP level 3 area to be enclosed by the 205°K isotherm.

At 1001 GMT (Fig. 17), the bands across the satellite image represent radiance data that were lost in transmission from the satellite. This is the time of greatest extent of the storm as measured by the area enclosed by the 210°K isotherm. It is seen that a small appendage of warm-cloud precipitation has developed on the south side of the system; otherwise, the relationships between the temperature values and echo intensities noted earlier still prevail. At this time the gust front on the western side of the storm is moving away from the precipitation area.

By 1202 GMT (Fig. 18) the storm is halfway in time between its time of maximum extent and its termination (the time when it ceased to qualify as an MCC). Figures 18 and 131 show that the gust front has now moved outside the 210°K isotherm on the east side of the system and even outside the satellite image on the west side. The good agreement between the 210°K isotherm and the VIP level 1 reflectivity region also has deteriorated somewhat.

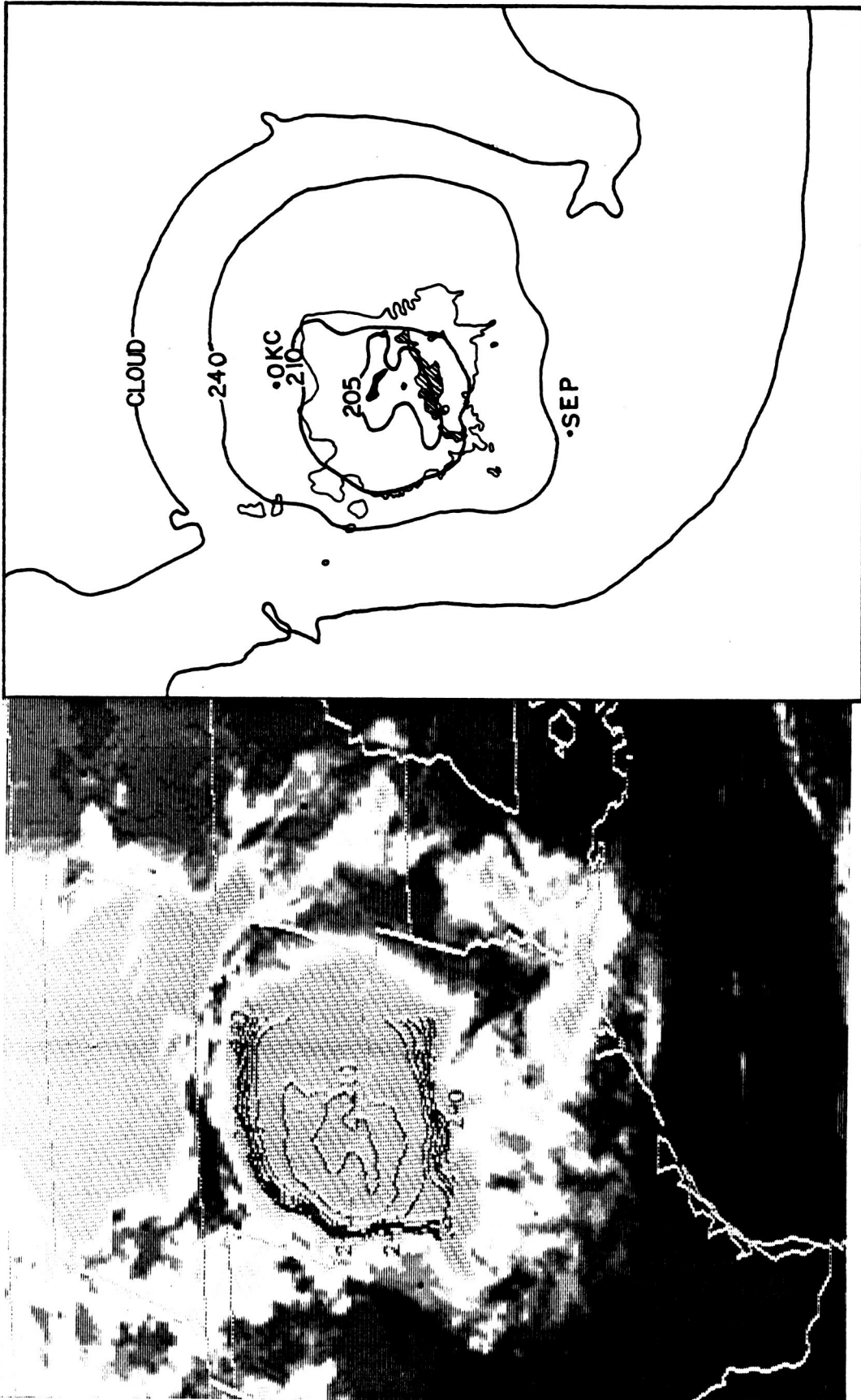


Fig. 15. Simultaneous views of satellite imagery and radar echoes at 0800 GMT. As in Fig. 14.

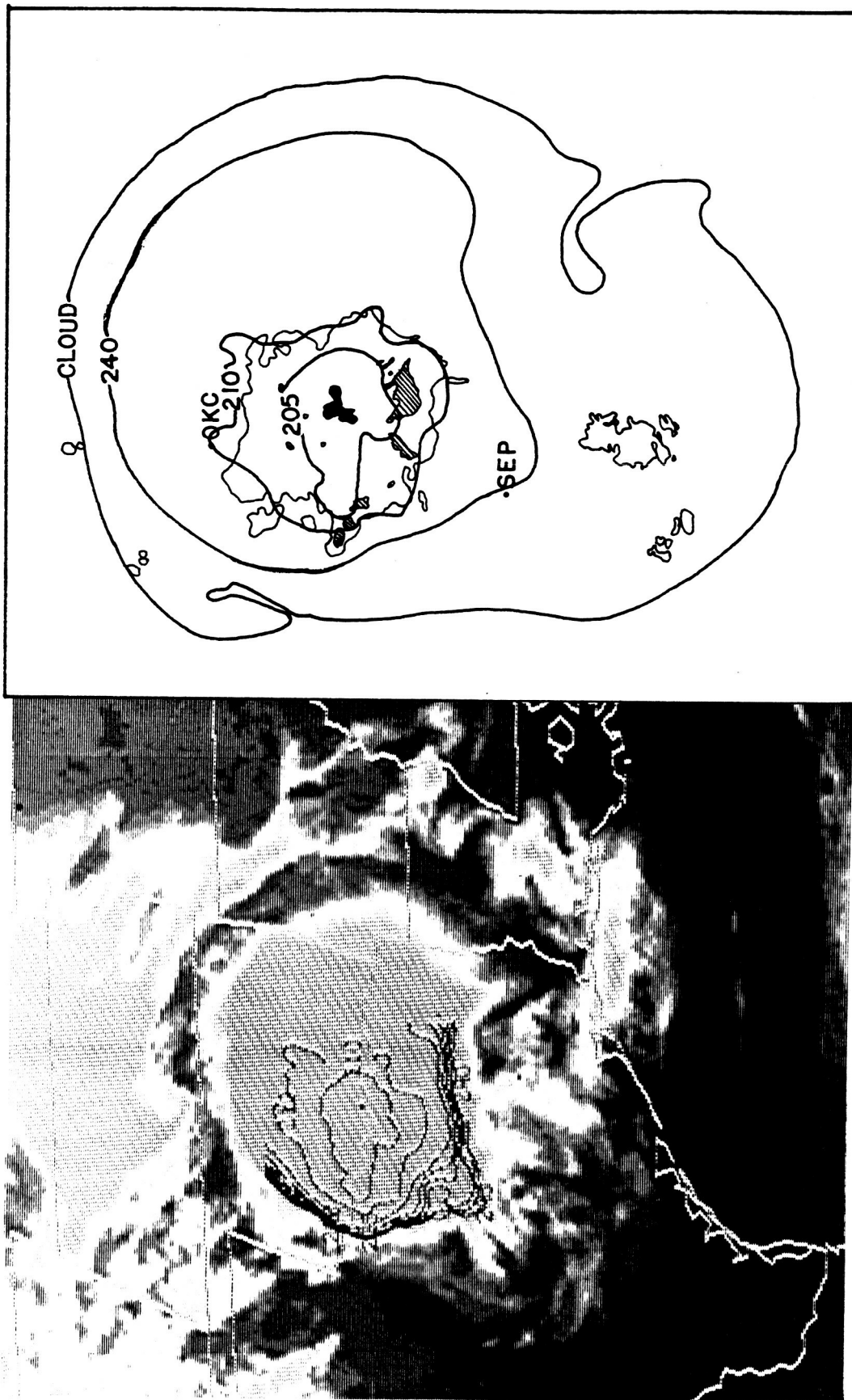


Fig. 16. Simultaneous views of satellite imagery and radar echoes at 0900 GMT. As in Fig. 14.

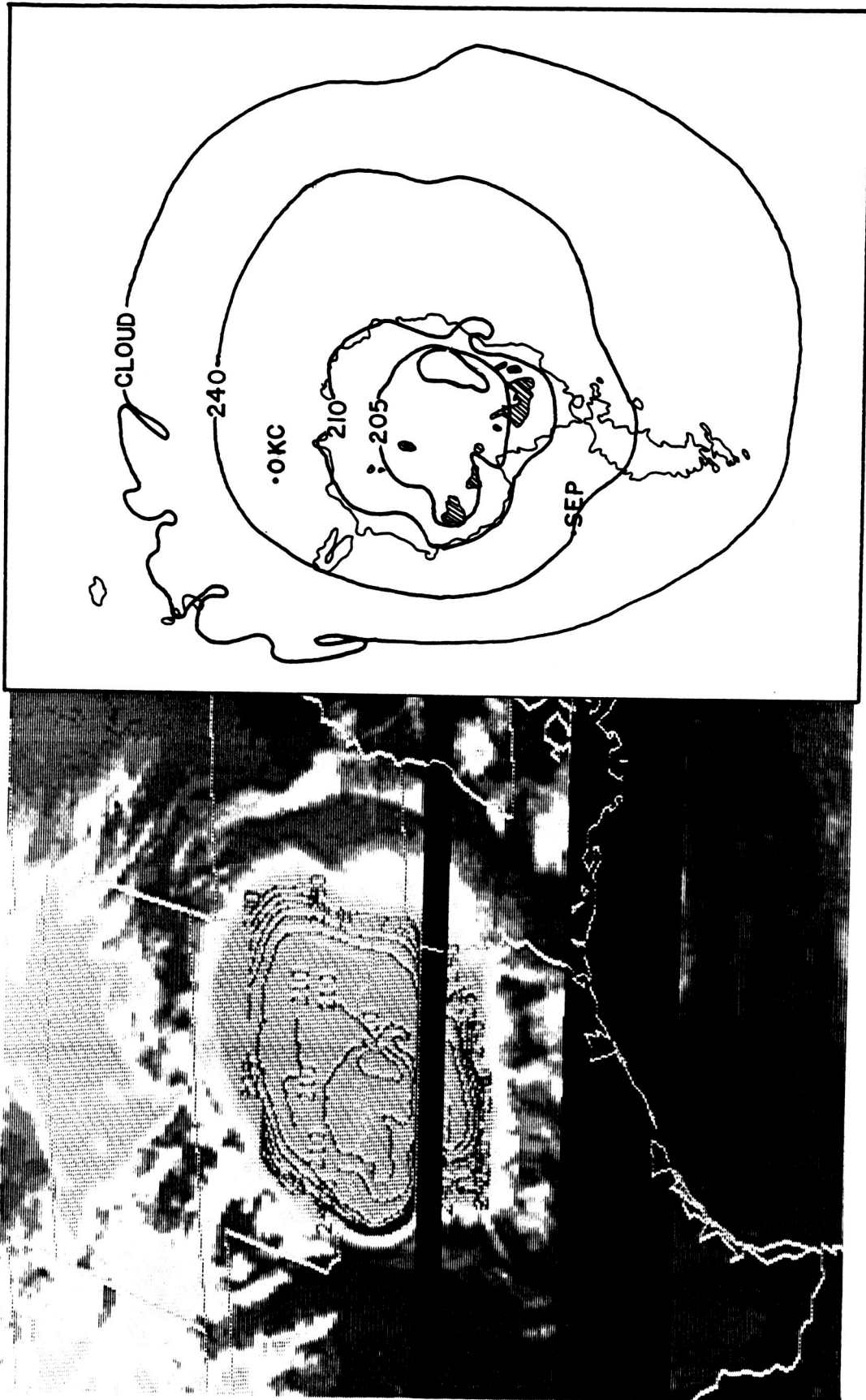


Fig. 17. Simultaneous views of satellite imagery and radar echoes at 1000 GMT. As in Fig. 14 except that some radiance data loss is indicated on the satellite image by black bands.

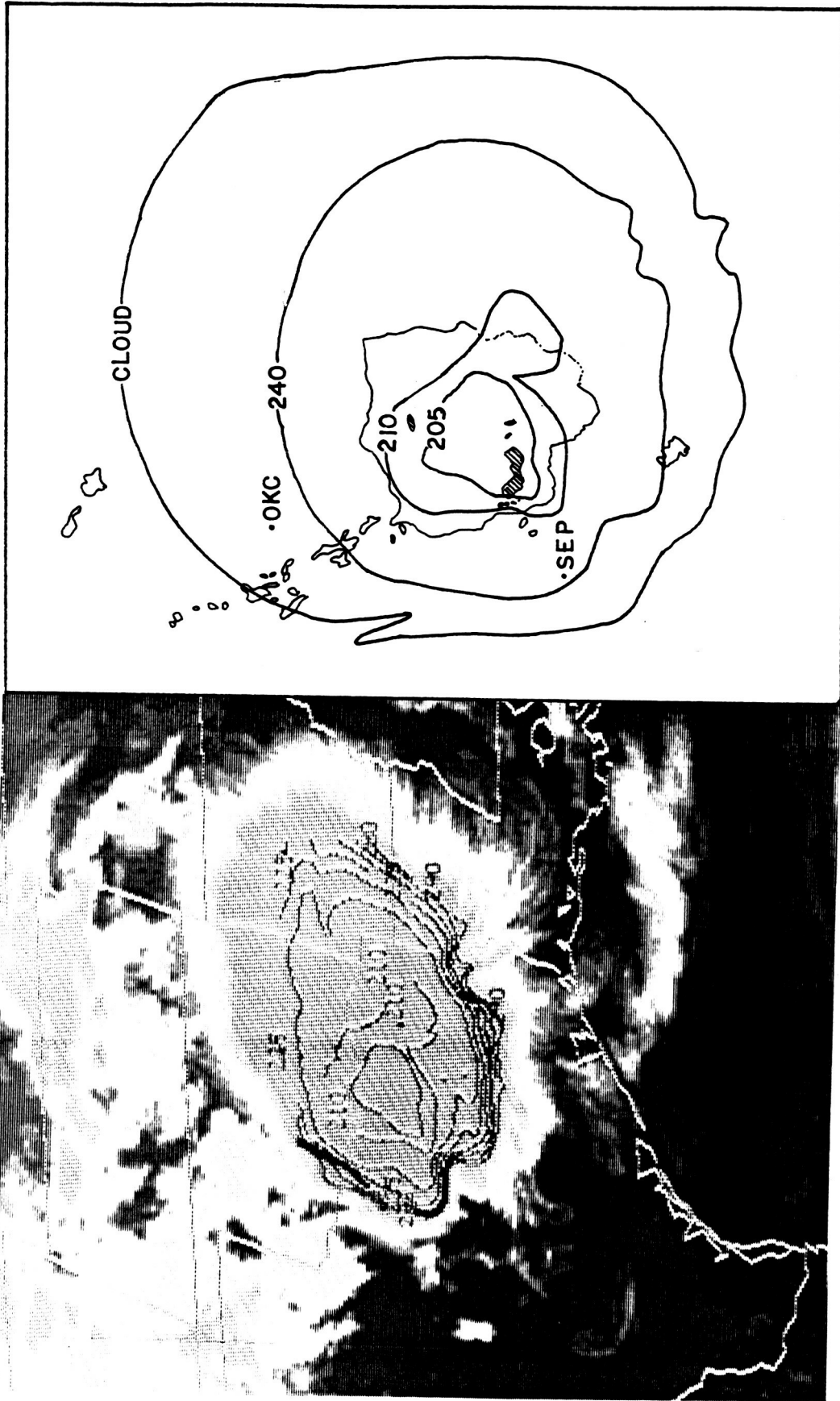


Fig. 13. Simultaneous views of satellite imagery and radar echoes at 1200 GMT. As in Fig. 14.

VIII. CONCLUSIONS AND RECOMMENDATIONS

The MCC of 27 May 1981 developed over southwestern Oklahoma and northern Texas and moved in a eastsoutheasterly direction. A synthesis of radar, satellite, sounding and surface data was used to determine the relationships between system and cell motions relative to the mean cloud layer wind, the relationship between cell development and the gust front, and the relationship between the rainfall patterns and amounts and cloud-top IR temperature structure.

Findings regarding the development and propagation of cells in an MCC are as follows:

- 1) The direction of cell (VIP level 3 or more reflectivity) propagation was found to be approximately the same as the system (VIP level 1 reflectivity) movement and the ambient wind.

- 2) Level 3 (or more) cells developed and dissipated on both the north and south ends of the line of maximum reflectivity. Thus, the system, as denoted by level 1 reflectivity, grew in size with time. Also, new cells developed to the rear of the line of maximum reflectivity as older cells continued their eastsoutheastward propagation. This led to a clockwise rotation of the line of maximum reflectivity. The resulting pattern of system and cell motion was not consistent with any of the models described by Marwitz (1972) for multi-cell systems.

- 3) Prior to its becoming an MCC the axis of maximum reflectivity was located near the center of the level 1 reflectivity. After MCC

initiation, this axis was observed to move to a position just behind the leading edge of the precipitation area. This agrees with results found by Leary and Rappaport (1983) using the combination of satellite imagery and radar echoes for an MCC in southwestern Texas. A gust front became identifiable in the surface synoptic data shortly after the initiation of the MCC. Its position in time was found to match well with the boundary of the precipitation area. Level 3 cells were found to form along or just inside the gust front and move with it. Later, as the gust front moved away from the precipitation area, further cell development ceased. These results imply that a synergistic relationship may exist between the system and the gust front in which the downdrafts and outflow from the MCC maintain the gust front, which in turn provides the convergence and updrafts to produce the cells.

Only a small portion of the storm area as seen in satellite imagery represents rainfall of sufficient intensity to be detected by radar. It was found that the 210°K isotherm in the IR satellite imagery tends to encompass this VIP level 1 region. Furthermore, the 205°K isotherm tends to surround a large portion of the heavier rainfall area as denoted by level 3 cells.

These generalizations are drawn from only one MCC and thus may not be representative of MCCs in different synoptic conditions, in different geographical regions, or earlier or later in the convective season.

It is obvious that a better, if not complete, understanding of the internal structure and dynamics of middle-latitude mesoscale systems can only be gained through an elaborate and specialized field study.

Fortunately, plans for such a study have been formulated (Zipser, 1984) and a preliminary, geographically- limited study has been carried out (Cunning, 1986) to test instrumentation and logistics. Until this field study can be accomplished, it is recommended that studies along the lines carried out here be continued. If the results found here can be confirmed, some understanding of MCCs will have been gained which may serve useful in the final planning of a large-scale field program.

REFERENCES

- Bartels, D. L., and A. A. Rockwood, 1983: Internal structure and evolution of a dual mesoscale convective complex. Preprints 5th Conf. Hydrometeorology, Tulsa, OK., Amer. Meteor. Soc., 97-102.
- Bosart, L. F., and F. Sanders, 1981: The Johnstown Flood of July 1977: A long-lived convective system. J. Atmos. Sci., 38, 1616-1642.
- Byers, H. R., and R. R. Braham, Jr., 1949: The Thunderstorm. U. S. Dept. of Commerce Weather Bureau, Washington, D C., 282pp.
- Cunning, J. B., 1986: The Oklahoma-Kansas preliminary regional experiment for STORM-Central. Bull. Amer. Meteor. Soc., 67, 1478-1486.
- Foster, D. S., and R. M. Reap, 1973: Archiving of manually digitized radar data. Techniques Development Laboratory Office Note 73-6, National Weather Service, Silver Springs, Md., 12pp.
- Fritsch, J. M., R. A. Maddox and A. G. Barnston, 1981: The character of mesoscale convective complex precipitation and its contribution to warm season rainfall in the United States. Preprints 4th Conf. Hydrometeorology, Reno, NV., Amer. Meteor. Soc., 94-99.
- Fujita, T., and H. A. Brown, 1958: A study of mesosystems and their radar echoes. Bull. Amer. Meteor. Soc., 39, 538-554.
- Gurka, J. J., 1976: Satellite and surface observations of strong wind zones accompanying thunderstorms. Mon. Wea. Rev., 104, 1484-1493.
- Heymsfield, G. M., and S. Schotz, 1985: Structure and evolution of severe squall line over Oklahoma. Mon. Wea. Rev., 113, 1563-1589.
- Howard, K. W., and R. A. Maddox, 1983: Precipitation characteristics of

- two mesoscale convective systems. Preprints 5th Conf. Hydrology, Tulsa, OK., Amer. Meteor. Soc., 11pp.
- Leary, C. A., and E. N. Rappaport, 1983: Internal structure of a mesoscale convective complex, Preprints 21st Conf. Radar Meteorology, Edmonton, Amer. Meteor. Soc., 70-77.
- Maddox, R. A., 1980a; A satellite based study of midlatitude, mesoscale convective complexes. Preprints 8th Conf. Weather Forecasting and Analysis, Denver, CO., Amer. Meteor. Soc., 329-338.
- , 1980b: Mesoscale convective complexes. Bull. Amer. Meteor. Soc., 61, 1374-1387.
- , D. M. Rodgers and K. W. Howard, 1982: Mesoscale convective complexes over the United States during 1981. Mon Wea. Rev., 110, 1501-1514.
- , and K. W. Howard, 1983: Simultaneous radar and satellite depictions of mesoscale convective systems. Preprints 5th Conf. Hydrometeorology, Tulsa, OK., Amer. Meteor. Soc., 10pp.
- McAnelly, R. L., and W. R. Cotton, 1986: Meso- β -scale characteristics of an episode of meso- α -scale convective complexes. Mon. Wea. Rev., 114, 1740-1770.
- Marwitz, J. D., 1972: The structure and motion of severe hailstorms. Part II: Multi-cell storms. J. Appl. Meteor., 11, 180-188.
- Merritt, J. H., and J. M. Fritsch, 1984: Convective complexes. Earth and Mineral Sciences, 54, 1-4.
- Miller, M. J., 1978: The Hampstead storm: A numerical simulation of a quasi-stationary cumulonimbus system. Quart. J. Roy. Meteor. Soc., 104, 413-427.

- Newton, C. W., and J. C. Fankhauser, 1975: Movement and propagation of multicellular convective storms. Pageogh., 113, 747-764.
- Purdom, J. F. W., 1973: Meso-highs and satellite imagery. Mon. Wea. Rev., 101, 180-181.
- , 1976: Some uses of high-resolution GOES imagery in the mesoscale forecasting of convection and its behavior. Mon. Wea. Rev., 104, 1474-1483.
- , 1979: The development and evolution of deep convection. Preprints 11th Conf. Severe Storms, Kansas City, MO., Amer. Meteor. Soc., 143-150.
- Rodgers, D. M., K. W. Howard and E. C. Johnston, 1983: Mesoscale convective complexes over the United States during 1982. Mon. Wea. Rev., 111, 2363-2369.
- , M. J. Magnano and J. H. Arns, 1985: Mesoscale convective complexes over the United States during 1983. Mon. Wea. Rev., 113, 888-901.
- Welshinger, M. J., 1985: Factors leading to the formation of arc cloud complexes. Masters Thesis, Texas A & M Univ., College Station, TX., 117 pp.
- Wilhelmson, R. B., and C. S. Chen 1982: A simulation of the development of successive cells along a cold outflow boundary. J. Atmos. Sci., 39, 1466-1483.
- Zehr, R. M. and James F. W. Purdom, 1982: Examples of a wide variety of thunderstorm propagation mechanisms. Preprints 12th Conf. Severe Storms, San Antonio, TX., Amer. Meteor. Soc., 499-502.
- Zipser, E. J., 1984: The national STORM program STORM-Central phase

preliminary program design. Prepared by the National Center for Atmospheric Research for the team for STORM-Central, Boulder, CO 80303.